ISSN 2658-3658

“Instrumentation Engineering, Electronics and Telecommunications – 2020”

Proceedings of the VI International Forum

December 2–4, 2020
Izhevsk, Russia

The Ministry of Education and Science of the Russian Federation
Kalashnikov Izhevsk State Technical University

“INSTRUMENTATION ENGINEERING, ELECTRONICS AND TELECOMMUNICATIONS - 2020”

Proceedings of the VI International Forum

(Izhevsk, Russia, December 2-4, 2020)

Publishing House
of Kalashnikov ISTU
Izhevsk 2020

UDC 681.2(06)

Instrumentation Engineering, Electronics and Telecommunications - 2020 : Proceedings of the VI International Forum (Izhevsk, Russia, December 2-4, 2020). - Izhevsk : Publishing House of Kalashnikov ISTU, 2020. - 41 p. - 4.1 Mb.

ISSN 2658-3658

This volume contains papers on wide range of problems in fields of instrumental engineering, electronics, telecommunications and related areas discussed during the VI International Forum "Instrumentation Engineering, Electronics and Telecommunications - 2020", IEET-2020, December 2-4, 2020, Izhevsk, Russia. All presented papers were selected after double-blind peer-rewiew. The Forum takes place annually in the Kalashnikov Izhevsk State Technical University.

UDC 681.2(06)

ISSN 2658-3658

Минобрнауки России
Федеральное государственное бюджетное образовательное
учреждение высшего образования
«Ижевский государственный технический университет имени М. Т. Калашникова»

«ПРИБОРОСТРОЕНИЕ, ЭЛЕКТРОНИКА И ТЕЛЕКОММУНИКАЦИИ – 2020»

Сборник статей VI Международного форума

(Россия, Ижевск, 2–4 декабря 2020 г.)

Издательство ИжГТУ
имени М. Т. Калашникова
Ижевск 2020

УДК 681.2(06)
П75

П75 **Приборостроение, электроника и телекоммуникации – 2020** [Электронный ресурс] : сб. ст. VI Междунар. форума (Россия, Ижевск, 2–4 декабря 2020 г.). – Ижевск : Изд-во ИжГТУ имени М. Т. Калашникова, 2020. – 41 с. – 4,1 Мб.

ISSN 2658-3658

Сборник содержит статьи на английском языке по широкому кругу вопросов в области приборостроения, электроники, связи и смежных им, которые обсуждались на VI Международном форуме “Instrumentation Engineering, Electronics and Telecommunications – 2020” («Приборостроение, электроника и телекоммуникации – 2020»), IEET-2020, 2–4 декабря 2020 года, Россия, г. Ижевск. Все представленные статьи были отобраны по результатам двойного слепого рецензирования. Форум проводится ежегодно в Ижевском государственном техническом университете имени М. Т. Калашникова.

УДК 681.2(06)

ISSN 2658-3658

TABLE OF CONTENTS

DOI: 10.22213/2658-3658-2020-6-11

Comparison of Methods for Determining the Physical Parameters of the Resonator of a Solid-State Wave Gyroscope

R. I. Mingazov [1], F. I. Spiridonov, I. A. Vikhlyaev, K. V. Shishakov

Radio Engineering Department of the Kalashnikov Izhevsk State Technical University
Izhevsk, Russian Federation
E-mail: ramzsjkee@gmail.com [1]

Received: July 15, 2020

Abstract. The article deals with the problem of identifying the dynamic parameters of the resonator of a solid-state wave gyroscope, based on the signals measured when the sensor is operating in free-run mode. The search for the dynamic parameters of a solid-state wave gyroscope is one of the most important operations of the quality control of its production. The paper describes two methods for determining the physical parameters of a quartz resonator of a solid-state wave gyroscope. For each method, the mathematical substantiation of the relationship between the dynamic behavior of the resonator and its physical parameters is given. On the basis of each of the techniques, an algorithmic support for the extraction of the physical parameters of the resonator of a solid-state wave gyroscope is presented. The research of the accuracy of calculating the visual parameters by the described methods on experimental data of a resonator with known parameters has been carried out. The results obtained show the practical applicability of the described methods. An example of using the methods described in the work is the identification and control of the dynamic parameters of a quartz hemispherical resonator of a solid-state wave gyroscope at the technological stage of "balancing".

Keywords: solid-state wave gyroscopes, dynamic parameters, conjugate gradient method, q-factor, different q-factor, different frequency, rigidity axes, viscosity axis

INTRODUCTION

Production cycle of hemispherical resonator gyroscope (HRG) includes a lot of technological operations, such as, operations of balancing control, different frequency, different Q-quality, calibration and others [1–3]. These operations control the most important parameters that affect the accuracy of the output signals of the HRG, are performed by measuring the dynamic characteristics of standing waves of a quartz resonator [4–9]. Since the latter characteristics turn out to be strongly related to the dynamic parameters of the TVG resonator, therefore, the research of the accuracy of the models for identifying the physical parameters of the resonator was chosen as the topic of this article.

THE PARAMETRIC STRUCTURE OF THE MEASURED SIGNALS

The wave processes observed by the measuring device have the following internal structure [1–3]:

$$\begin{aligned} C(t) &= A(t)\cos\theta(t)\cos(2\pi\omega t+\varphi) - B(t)\sin\theta(t)\sin(2\pi\omega t+\varphi),\\ S(t) &= A(t)\sin\theta(t)\cos(2\pi\omega t+\varphi) + B(t)\cos\theta(t)\sin(2\pi\omega t+\varphi), \end{aligned} \tag{1}$$

where $A(t)$ – amplitude of the main vibrations, $B(t)$ – amplitude of the quadrature oscillations, $\theta(t)$ – angular orientation of the wave, $\omega(t)$ – average oscillation frequency, φ – initial phase displacement.

In the general case, these functions depend not only on time t, but also on the physical parameters of the HRG resonator:

$$\begin{aligned} A(t) &= \tilde{A}(\eta, \Delta\eta, \vartheta_\eta, \Delta\nu, \vartheta_\nu, t),\\ B(t) &= \tilde{B}(\eta, \Delta\eta, \vartheta_\eta, \Delta\nu, \vartheta_\nu, t),\\ \theta(t) &= \tilde{\theta}(\eta, \Delta\eta, \vartheta_\eta, \Delta\nu, \vartheta_\nu, t). \end{aligned}$$

where η – damping factor, $\Delta\eta$ – delta of the damping factor, θ_η – axis of maximum viscosity, $\Delta\nu$ – value of different frequency, and θ_ν – axis of maximum stiffness.

The mathematical model of the rate of change of variables in the free-coast mode (without control action) is described by the equations [9–11]:

$$\begin{aligned} \dot{A}(\eta, \Delta\eta, \vartheta_\eta, \Delta\nu, \vartheta_\nu, t) &= -\eta A(t) - 2\Delta\eta A(t)\cos 2(\theta(t)-\vartheta_\eta) - \Delta\nu B(t)\sin 2(\theta(t)-\vartheta_\nu),\\ \dot{B}(\eta, \Delta\eta, \vartheta_\eta, \Delta\nu, \vartheta_\nu, t) &= -\eta B(t) + 2\Delta\eta B(t)\cos 2(\theta(t)-\vartheta_\eta) + \Delta\nu A(t)\sin 2(\theta(t)-\vartheta_\nu),\\ \dot{\theta}(\eta, \Delta\eta, \vartheta_\eta, \Delta\nu, \vartheta_\nu, t) &= \frac{(-\Delta\eta(\sin 2\theta(t)\cos 2\vartheta_\eta + \cos 2\theta(t)\sin 2\vartheta_\eta) - g_3)A(t)^2}{A(t)^2 - B(t)^2} + \\ &+ \frac{(-\Delta\eta(\sin 2\theta(t)\cos 2\vartheta_\eta + \cos 2\theta(t)\sin 2\vartheta_\eta) + g_3)B(t)^2}{A(t)^2 - B(t)^2} + \\ &+ \frac{2\Delta\nu(\cos 2\theta(t)\cos 2\vartheta_\nu + \sin 2\theta(t)\sin 2\vartheta_\nu)A(t)B(t)}{A(t)^2 - B(t)^2}, \end{aligned} \tag{2}$$

or

$$\begin{aligned} \dot{A}(\eta, \Delta\eta, \vartheta_\eta, \Delta\nu, \vartheta_\nu, t) &= -\eta A(t) - 2\Delta\eta_c A(t)\cos 2\theta - 2\Delta\eta_s A(t)\sin 2\theta - \\ &- \Delta\nu_c B(t)\sin 2\theta + \Delta\nu_s B(t)\cos 2\theta,\\ \dot{B}(\eta, \Delta\eta, \vartheta_\eta, \Delta\nu, \vartheta_\nu, t) &= -\eta B(t) + 2\Delta\eta_c B(t)\cos 2\theta + 2\Delta\eta_s B(t)\sin 2\theta + \\ &+ \Delta\nu_c A(t)\sin 2\theta - \Delta\nu_s A(t)\cos 2\theta,\\ \dot{\theta}(\eta, \Delta\eta, \vartheta_\eta, \Delta\nu, \vartheta_\nu, t) &= \frac{(-\sin 2\theta(t)\Delta\eta_c + \cos 2\theta(t)\Delta\eta_s - g_3)A(t)^2}{A(t)^2 - B(t)^2} + \\ &+ \frac{(-\sin 2\theta(t)\Delta\eta_c + \cos 2\theta(t)\Delta\eta_s + g_3)B(t)^2}{A(t)^2 - B(t)^2} + \\ &+ \frac{2(\cos 2\theta(t)\Delta\nu_c + \sin 2\theta(t)\Delta\nu_s)A(t)B(t)}{A(t)^2 - B(t)^2}, \end{aligned} \tag{3}$$

where $\Delta\eta_c = \Delta\eta \cos 2\theta_\eta$, $\Delta\eta_s = \Delta\eta \sin 2\theta_\eta$, $\Delta\nu_c = \Delta\nu \cos 2\theta_\nu$, $\Delta\nu_s = \Delta\nu \sin 2\theta_\nu$.

CALCULATION OF THE PARAMETERS OF THE RESONATOR BY OBSERVING THE COAST

Substituting all derivatives in (3) with first-order difference schemes on the sampling interval T:

$$\begin{aligned}
\frac{A^{i+1}-A^{i}}{T} &= -\eta A^{i+1/2} - 2\Delta\eta_c A^{i+1/2}\cos 2\theta^{i+1/2} - 2\Delta\eta_s A^{i+1/2}\sin 2\theta^{i+1/2} - \\
&\quad - \Delta\nu_c B^{i+1/2}\sin 2\theta^{i+1/2} + \Delta\nu_s B^{i+1/2}\cos 2\theta^{i+1/2}, \\
\frac{B^{i+1}-B^{i}}{T} &= -\eta B^{i+1/2} + 2\Delta\eta_c B^{i+1/2}\cos 2\theta^{i+1/2} + 2\Delta\eta_s B^{i+1/2}\sin 2\theta^{i+1/2} + \\
&\quad + \Delta\nu_c A^{i+1/2}\sin 2\theta^{i+1/2} - \Delta\nu_s A^{i+1/2}\cos 2\theta^{i+1/2}, \\
\frac{\theta^{i+1}-\theta^{i}}{T} &= \frac{(-\sin(2\theta^{i+1/2})\Delta\eta_c + \cos(2\theta^{i+1/2})\Delta\eta_s - g_3)A^{i+1/2}\cdot A^{i+1/2}}{A^{i+1/2}A^{i+1/2} - B^{i+1/2}B^{i+1/2}} \\
&\quad + \frac{(-\sin(2\theta^{i+1/2})\Delta\eta_c + \cos(2\theta^{i+1/2})\Delta\eta_s + g_3)B^{i+1/2}\cdot B^{i+1/2}}{A^{i+1/2}A^{i+1/2} - B^{i+1/2}B^{i+1/2}} \\
&\quad + \frac{2(\cos(2\theta^{i+1/2})\Delta\nu_c + \sin(2\theta^{i+1/2})\Delta\nu_s)A^{i+1/2}B^{i+1/2}}{A^{i+1/2}A^{i+1/2} - B^{i+1/2}B^{i+1/2}}.
\end{aligned} \tag{4}$$

where the left and right sides of (4) are taken from the observed quantities {A, B, theta}.

After the left side of the equation system are collected in the vector dimension $\mathbf{h}(N, 1)$, right in the matrix $\mathbf{M}(N, 5)$ and the unknown vector is denoted $\mathbf{r} = [\eta, \Delta\eta_c, \Delta\eta_s, \Delta\nu_c, \Delta\nu_s]$, the system (4) can be written in matrix form [9]:

$$\mathbf{h} = \mathbf{M}\times\mathbf{r}. \tag{5}$$

Since the system of equations (5) is redundant, its solution is possible through minimization of the residual. This leads to the matrix equation:

$$\mathbf{M}^{\mathrm{T}}\times\mathbf{h} = \mathbf{M}^{\mathrm{T}}\times\mathbf{M}\times\mathbf{r} \Rightarrow \mathbf{r} = \left(\mathbf{M}^{\mathrm{T}}\times\mathbf{M}\right)^{-1}\times\mathbf{M}^{\mathrm{T}}\times\mathbf{h}. \tag{6}$$

To find the parameters of the HRG in coasting mode remains the problem of finding the wave variables.

NUMERICAL CALCULATION OF WAVE VARIABLES

In equation (1) the basic information functions are A(t), $B(t)$, $\theta(t)$, which is found by minimizing the functional errors:

$$\begin{gathered}
F = \sum_i \begin{pmatrix} \left[-C_i + A_i\cos\theta_i\cos(\tau_i) - B_i\sin\theta_i\sin(\tau_i)\right]^2 + \\ +\left[-S_i + A_i\sin\theta_i\cos(\tau_i) + B_i\cos\theta_i\sin(\tau_i)\right]^2 \end{pmatrix} \to 0, \\
\tau_i = 2(\pi\omega)_i\cdot i\cdot n + \varphi_i, \quad i = 0...N.
\end{gathered} \tag{7}$$

To numerically minimize it by the vector of parameters, the conjugate gradient method was chosen.

TRANSITION TO NEW VARIABLES (p, q, r).

The calculation of the variables [A, B, θ] can be simplified by introducing the following new variables [8]:

$$cc = \frac{2}{N}\sum_i C_i C_i = A^2\cos^2(\theta) + B^2\sin^2(\theta) = \frac{1}{2}(A^2 + B^2) + \frac{1}{2}(A^2 - B^2)\cos(2\theta),$$
$$cs = \frac{2}{N}\sum_i C_i S_i = (A^2 - B^2)\sin(\theta)\cos(\theta) = \frac{1}{2}(A^2 - B^2)\sin(2\theta), \quad (8)$$
$$ss = \frac{2}{N}\sum_i S_i S_i = A^2\sin^2(\theta) + B^2\cos^2(\theta) = \frac{1}{2}(A^2 + B^2) - \frac{1}{2}(A^2 - B^2)\cos(2\theta),$$

Next we proceed from basis [A, B, θ] to a new basis:

$$p = cc - ss = (A^2 - B^2)\cos(2\theta),$$
$$q = 2cs = (A^2 - B^2)\sin(2\theta), \quad (9)$$
$$r = cc + ss = A^2 + B^2.$$

As a result, equations (3) will take the form:

$$\dot{p} = 2\eta p + 2g_3 q + 2\Delta\eta_c r - 4AB\Delta\nu_s,$$
$$\dot{q} = -2g_3 p + 2\eta q + 2\Delta\eta_s r + 4AB\Delta\nu_c, \quad (10)$$
$$\dot{r} = 2\Delta\eta_c p + 2\Delta\eta_s q + 2\eta r,$$

where AB = sign(B)·sqrt($r^2 - p^2 - q^2$), as well as g_3 the projection of rotation rate of the earth.

Further, the system of equations (10) performed substitution derivatives on time-difference scheme first order in analogy to (4). The resulting system of equations is solved by analogy with (5), (6). And the result of its solution will be a vector [η, $\Delta\eta_c$, $\Delta\eta_s$, $\Delta\nu_c$, $\Delta\nu_s$].

At the last phase of computations, the values of physical parameters are calculated using its values using the following formulas:

$$\vartheta_\eta = \frac{1}{4}\arctan\left(\frac{\Delta\eta_s}{\Delta\eta_c}\right),\ \vartheta_\nu = \frac{1}{4}\arctan\left(\frac{\Delta\nu_s}{\Delta\nu_c}\right),$$
$$Q = \frac{\pi\omega}{\eta},\ \Delta Q = \frac{\pi\omega}{\sqrt{\Delta\eta_c{}^2 + \Delta\eta_s{}^2}},\ \Delta\nu = \sqrt{\Delta\nu_c{}^2 + \Delta\nu_s{}^2}. \quad (11)$$

where θ_η – axis of maximum viscosity, θ_ν – axis of maximum stiffness, Q – Q-factor, ΔQ – varied Q-factor, $\Delta\nu$ – different frequency.

COMPARISON OF CALCULATION RESULTS

HRG dynamic parameters were calculated by two methods according to formula (11). The math package Scilab was used for calculations.

In the first method, first solved (7), then from equation (4) is constructed in the matrix equation (5) and at the end, a system of equations (6).

In the second method, first phase variables are calculated by formulas (8), (9), then system (5) is constructed and the system of equations (6) is solved.

For an example of calculating the parameters of the HRG resonator, the data obtained experimentally at the stand for balancing are used. The initial data were obtained from the HRG resonator in the form of signals (C, S) (1), the measurement time was 60 sec, the sampling frequency of the ADC was 33333 Hz.

Table 1 shows the results of calculating the parameters of the resonator. The calculation of one value of a slowly varying variable was carried out for 1 period of oscillations.

Table 1. Result of HRG resonator calculation

Parameters	**Ideal value**	**Through the identification of A, B, θ (1^{st} method)**	**By calculating p, q, r (2^{nd} method)**
Q-factor	4210350.328	4196531.783	4193124.846
Varied Q-factor (%)	7	7.21	2.96
Axis of maximum viscosity, Degrees	88.9	89.0547	86.654
Different frequency, Hz	0.0003	0.0002734	0.0005286
Axis of maximum stiffness, Degrees	61.4	60.9435	59.9534

CONCLUSION

In this paper, mathematical models for determining the parameters of the resonator of a solid-state wave gyroscope are considered. Two computational methods for revealing the resonator parameters are analyzed. Each method has its own pros and cons. For example, the method based on the numerical minimization of the error functional by the least squares method has a higher accuracy than the method for calculating the values of p, q, r. Moreover, the second method has a lower computational complexity in comparison with the method of minimizing the error functional. It is also worth noting that the calculation of the parameters p, q, r should be performed over the full period of resonator oscillations.

These algorithms for identifying the parameters of the resonator of a solid-state wave gyroscope can be widely used in the production of gyroscopic devices and devices based on it. For example, in such technological operations as: balancing, tuning and control.

REFERENCES

1. Matveev, V. A., Lipatnikov, V. I., & Alehin, A. V. (1997). *Proektirovanie volnovogo tverdotelnogo giroskopa [Designing of hemispherical resonator gyroscope]*. Moscow, Russia : MGTU im. N. E. Baumana. (in Russian).
2. Lunin, B. S., Matveev, V. A., & Basarab, M. A. (2014). *Volnovoj tverdotel'nyj giroskop. Teorija i tehnologija [Hemispherical resonator gyro. Theory and technology]*. Moscow, Russia : Radiotehnika, 176 pp. (in Russian).
3. Shishakov, K. V. (2018). *Tverdotel'nye volnovye giroskopy: volnovye processy, upravlenie, sistemnaja integracija [Solid-state wave gyroscopes: wave processes, control, system integration]*. Izhevsk, Russia : Publ. House of Izhevsk State Technical University. (in Russian).
4. Zhbanov, Yu. K., & Kalenova, N. V. (2001). Surface unbalance of a hemispherical resonator gyro. *Mechanics of Solids, 36*(3), 7-12.

5. Maslov, A. A., Maslov, D. A., & Merkurev, I. V. (2014). Identifikatsiya parametrov volnovogo tverdotel'nogo giroskopa s uchetom nelineynosti kolebaniy rezonatora [Parameter identification of hemispherical resonator gyro woth nonlinearity of the resonator]. *Pribory i sistemy. Upravlenie, kontrol', diagnostika [Instruments and Systems. Monitoring, Control, and Diagnostics],* (5), 18-23. (in Russian).
6. Levshonkov, N. V. (2013). Metody vesovoj balansirovki rotora sverhlegkogo vertoleta s soosnymi vintami [Methods of mass balancing an ultralight helicopter rotor with coaxial screws]. *Vestnik Kazanskogo gosudarstvennogo technichecskogo universiteta im. A.N. Tupoleva [Bulletin of Tupolev KSTU],* (2-1), 5-7. (in Russian).
7. Krivov, A. V., & Abramov, I. V. (2016). Sovremennoe sostoyanie problem balansirovki rezonatorov tverdotelnogo volnovogo giroskopa [Current state of the problem of balancing resonators of a hemispherical resonator gyroscope]. In *Molodye uchenye - uskoreniyu nauchno-technicheskogo progressa v XXI veke: 20-21 Apr., 2016* (pp. 195-200). Izhevsk, Russia : INNOVA. (in Russian).
8. Zhuravlev, V. F. (2016). Dvumernyy ostsillyator Van der Polya c vneshnim upravleniem [Van der Pol's controlled 2D oscillator]. *Nelineynaya dinamika [Russian Journal of Nonlinear Dynamics], 12*(2), 211-222. (in Russian). doi: 10.20537/nd1602004.
9. Krivov, A. V., Melnikov, R. V., Spiridonov, F. I., & Trutnev, G. A. (2019). Opredelenie parametrov rezonatora tverdotel'nogo volnovogo giroskopa i modelirovanie po eksperimental'nym dannym [Determination of parameters of HRG resonator and experimental data modeling]. *Vestnik Kazanskogo gosudarstvennogo technichecskogo universiteta im. A.N. Tupoleva [Bulletin of Tupolev KSTU], 75*(2), 127-133. (in Russian).
10. Klimov, D. M., Zhuravlev, V. F., & Zhbanov, Y. K. (2017). *Kvartsevyi polusfericheskii resonator (Volnovoi tverdotel'nyi giroskop) [Quartz hemispherical resonator (Hemispherical resonator gyroscope)].* Moscow, Russia : Kim L. A. (in Russian).
11. Trutnev, G. A. (2015). The model of hemispherical resonator gyroscope in terms of slow variables [Model' tverdotel'nogo volnovogo giroskopa v medlennykh peremennykh]. *Vestnik Udmurtskogo Universiteta. Matematika. Mekhanika. Komp'yuternye Nauki [Bulletin of Udmurt University. Mathematics, Mechanics, Computer Science], 25*(3), 421-429. (in Russian). doi: 10.20537/vm150312.

DOI: 10.22213/2658-3658-2020-12-23

The Propagation of Antisymmetric Lamb Wave in the Hollow Cylinder

Yu. V. Myshkin [1], O. V. Muravieva [1,2], S. Yu. Voronchikhin [3], A. A. Pon'kina [1], S. A. Korolev [1]

[1] Department of Instruments and Techniques of Measurements, Testing, Diagnostics, Kalashnikov Izhevsk State Technical University, Izhevsk, Russian Federation
[2] Udmurt Federal Research Center of Ural Branch of the Russian Academy of Sciences, Izhevsk, Russian Federation
[3] IntroScan Technology JSC, Chaykovsky, Perm Krai, Russian Federation
E-mail: mubm@yandex.ru

Received: August 16, 2020

Abstract. The article presents research on the propagation of an antisymmetric Lamb wave mode in a hollow steel cylinder with an outer diameter of 1020 mm and a wall thickness of 16 mm at frequencies of 50 and 120 kHz. Dispersion curves for a pipe and a plate are given, examples of which show their similarity in the frequency range from 5 kHz and the presence of higher-order modes. Experimental studies were carried out using piezoelectric transducers with dry point contact on a spiral welded pipe. The research results showed the combined effect of the geometric anisotropy and anisotropy of the pipe material properties on the propagation velocity of the antisymmetric Lamb wave mode. The maximum difference in velocity depending on the angle of deviation of the wave propagation trajectory (deviation angle) was 35 and 55 m/s at a frequency of 50 and 120 kHz, respectively. The effect of the pipe wall thickness on the character of the dependence of the velocity on the deviation angle in the presence of dispersion was established, which amounted to 20 m/s per 1 mm of wall thickness for a given pipe geometry. A qualitative description of the formation of the shape of the dependence of the wave velocity on the deviation angle, which has a minimum at 30 degrees and a maximum at 90 degrees, is presented.

Keywords: Lamb wave, hollow cylinder, wave velocity, experimental study, dry point contact, guided wave testing, geometric anisotropy, spiral welded pipe.

INTRODUCTION

Modern methods of non-destructive testing make it possible to simultaneously detect defects, carry out thickness measurement and evaluate the structure of the material (structural health monitoring) [1-14]. One of these methods is acoustic guided wave testing, based on the use of guided waves, in particular, horizontally polarized shear wave, symmetric and antisymmetric Lamb wave modes. The choice of the type of wave during acoustic guided wave testing depends on its features: the presence of velocity dispersion; sensitivity to orientation, shapes and types of defects; applicability to the geometry of the testing object; properties of the material of the testing object, etc. [10-14]

The antisymmetric Lamb wave mode has not been widely used in the detection of defects due to the high dispersion of the velocity. However, this type of wave, along with resonance methods, is convenient to use for determining the dimensions of the thickness of plates and pipe walls. Using several emitters and receivers and algorithms for synthetic or active focusing, it is also used to determine the coordinates of local thinning of the walls of the pipe or plates [15-20]. Due to the high dispersion of the velocity of Lamb waves, these techniques allow them to be used in monitoring the structure and properties of a material [21-24], acoustic tomography [25-29], monitoring layered structures made of composite materials [20, 30-33], study of attenuation on discontinuities in plates [31, 34-36].

As a rule, when studying the processes of propagation of Lamb waves and evaluating research results, the following methods are used: the semi-analytical method of finite elements [37], the method of finite elements [18, 31, 35, 38, 39], Legendre spectral element method [22], dispersion ultrasound vibrometry method [24], spectral analysis [32], analytical methods [40,41], experimental experiments [23, 39]. To excite Lamb waves, the following methods and transducers are used: piezoelectric transducers [16, 17, 21, 42], electromagnetic-acoustic transducers [27, 43, 44], laser method [23, 45, 46], air-coupled transducers [39, 47, 48]. In research and practical use, the antisymmetric Lamb wave mode often becomes an interfering factor in the interpretation of testing results [19, 43].

When testing pipe wall thickness using an antisymmetric Lamb wave mode, the analysis of the results becomes more difficult, since all guided wave types are influenced by both the anisotropy of the pipe material properties and the geometric anisotropy. Studies on the influence of geometric anisotropy on the propagation velocity of the symmetric Lamb wave mode and the horizontally polarized shear wave are presented in [49-51]. Geometric anisotropy can change the wave velocity depending on the pipe geometry within the range up to 300 m/s from the calculated theoretical value.

The article presents the results of studies on the influence of geometric anisotropy and the anisotropy of the pipe material properties on the propagation velocity of the antisymmetric Lamb wave mode in a spiral welded pipe with diameter of 1020 mm and a wall thickness of 16 mm.

DISPERSION CURVES

Dispersion curves of phase and group velocities calculated in the Elastic Waveguide Tracer program were obtained for the pipe of the specified geometry (figure 1). For comparison, dispersion curves for a 16 mm thick plate are also shown (figure 2). The parameters for calculating the curves are given in the table 1. Since the experimental studies used transducers operating at a frequency of 50 and 120 kHz, then the velocities of all types of waves were calculated for them, which are presented in the table 2 and table 3 respectively. From the presented dispersion curves (figure 1 and figure 2) and the results of calculating the velocity (table 2 and table 3), it can be seen that the differences in the group and phase velocities for the pipe and plate are insignificant in the frequency range from 5 kHz and more. The main difference lies in the presence of higher-order modes in pipes at high frequencies, propagating at the same velocity as waves in the plate, and having distinctive diagrams of displacement components along the pipe wall thickness.

It can be seen from the velocities calculated from the dispersion curves that the velocity of the antisymmetric Lamb wave mode does not differ much from the velocity of the horizontally polarized shear wave. In particular, at 120 kHz, the velocities are practically the same. However, two types of waves can be distinguished by the direction of particle oscillations in the displacement diagram, since the horizontal component of displacements prevails in the

horizontally polarized shear wave, and in the antisymmetric Lamb wave mode, the normal component of displacements prevails.

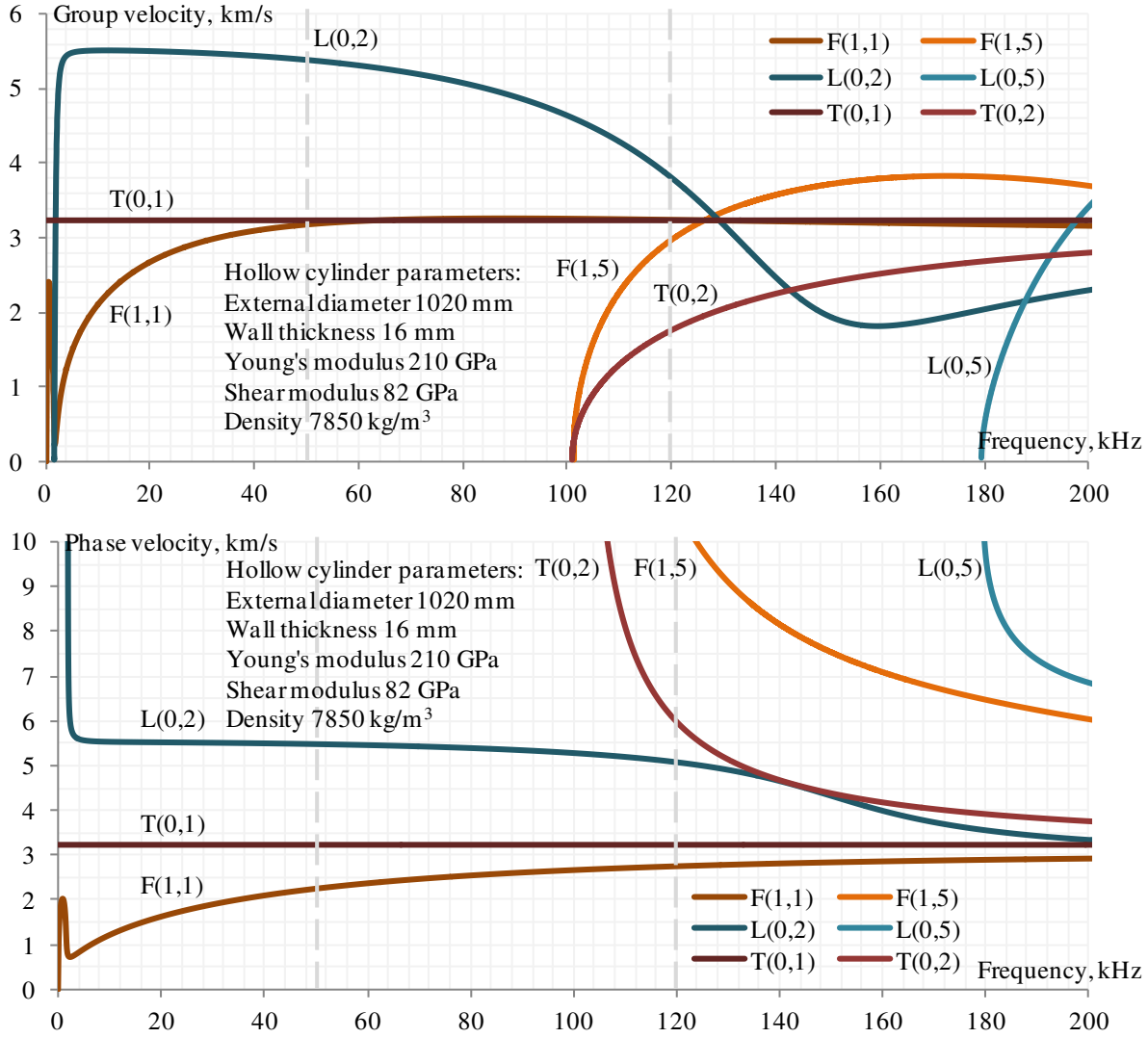

Figure 1. Dispersion curves of group and phase velocities in a steel hollow cylinder (b):
L – longitudinal wave, F – flexural wave, T – torsional wave

Table 1. Geometric and material properties

Parameter	Value	Dimension	Parameter	Value	Dimension
External radius	510	mm	Shear modulus, *G*	82	GPa
Wall thickness	16	mm	Poisson's ratio, η	0.28	-
Internal radius	494	mm	Shear wave velocity, *C*	3243	m/s
Young's modulus, *E*	210	GPa	Density, ρ	7850	kg/m^3

Table 2. Group velocities at the frequency of 50 kHz

Mode in plate	Group velocity (m/s)	Mode in pipe	Group velocity (m/s)
A0	3181	F(1,1)	3179
S0	5391	L(0,2)	5391
SH0	3242	T(0,1)	3242

Table 3. Group velocities at the frequency of 120 kHz

Mode in plate	Group velocity (m/s)	Mode in pipe	Group velocity (m/s)
A0, A1	3242, 2976	F(1,1), F(1,5)	3242, 2979
S0	3809	L(0,2)	3810
SH0, SH1	3242, 1746	T(0,1), T(0,2)	3242, 1746

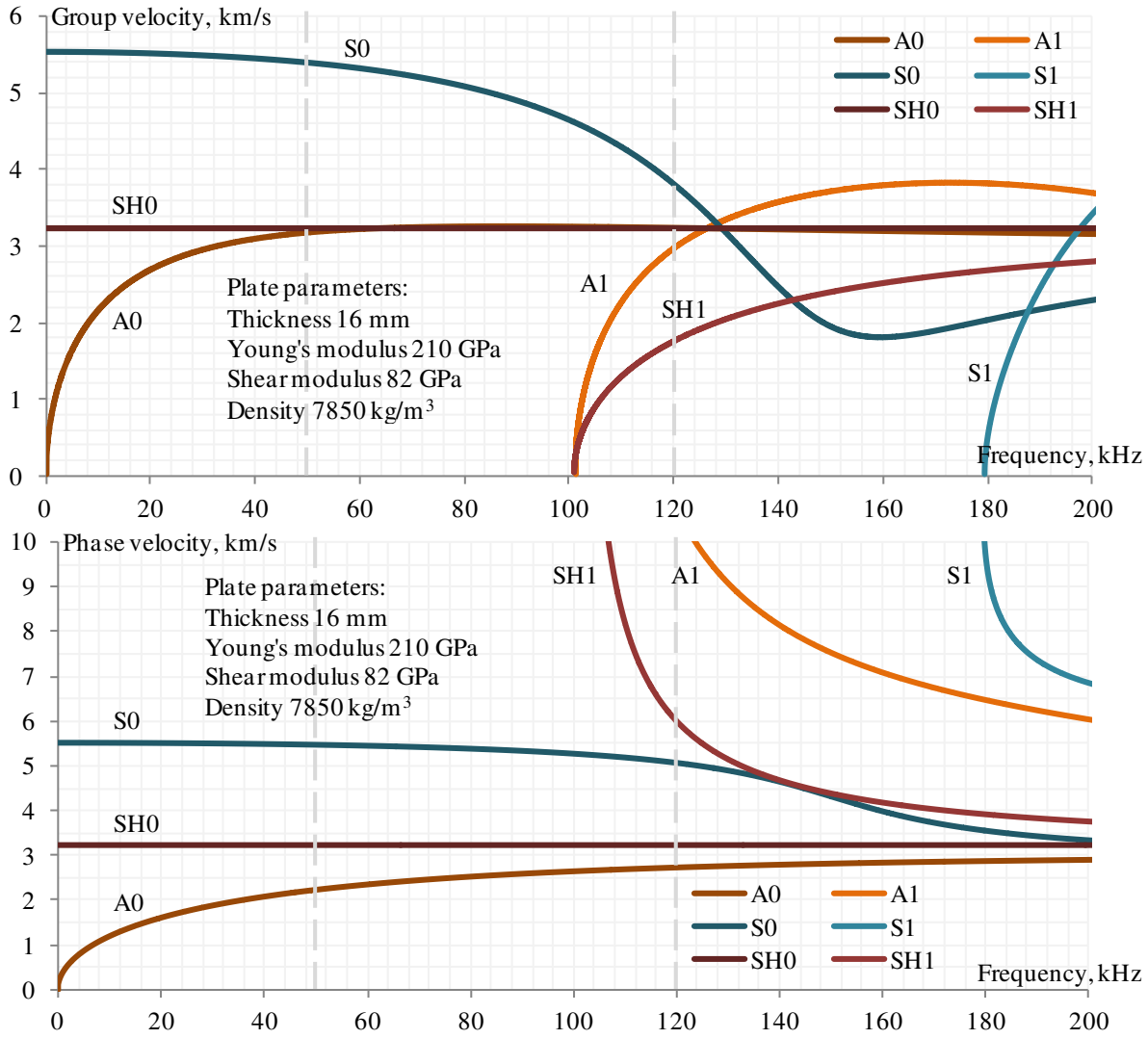

Figure 2. Dispersion curves of group and phase velocities in a steel plate: S – symmetrical mode of Lamb wave, A – antisymmetrical mode of Lamb wave, SH – horizontally polarized shear wave

To separate wave types in experimental studies, specialized designs and orientations of transducers were used, which made it possible to create tangential or normal displacements on the surface of the testing object.

Experimental Setup

The experimental setup included a stand consisting of a system of pipelines of various diameters, two piezoelectric transducers with dry point contact, and a DIO-1000LF flaw detector (figure 3). A pipeline with a diameter of 1020 mm was marked on the outside with

a specialized template in such a way that the points for installing the receiving transducer were located at a distance of 1 m from the point of installing the emitter with a step of 1 degree. The marking and measurements were carried out in one quadrant in the range of angles from 0 to 90 degrees, while the direction along the axis along the pipe generatrix was taken as 0 degrees. As already noted, for the excitation and reception of the antisymmetric Lamb wave mode, the normal component of the displacements was used, created and recorded by piezoelectric transducers with dry point contact.

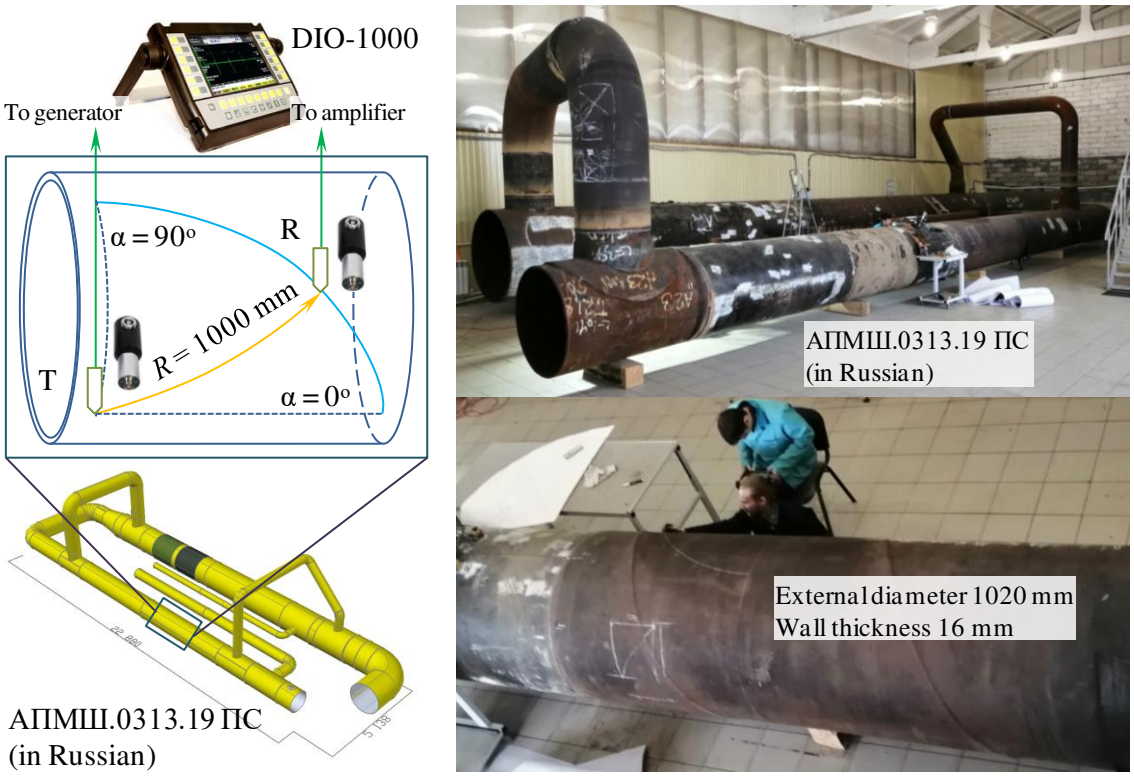

Figure 3. A scheme and photo of the experimental setup: α – deviation angle – angle of deviation of the path of wave propagation from pipe generatrix, T – transmitter, R – receiver

As a result of measurement, the figure 4 shows an echogram at the point of reception of oscillations of a signal transmitted once from the transmitter to the receiver. To increase the accuracy of calculating the wave velocity, the range of the recorded signal was limited by the window including the beginning (310 μs) and end (400 μs) of the echo pulse of the antisymmetric Lamb wave mode, while the signal sampling rate was 200 MHz.

For the time of arrival of the pulse (time of flight), the average value of the time, the observed maxima and minima in the limited window of the recorded signal was taken, which made it possible to detach from the influence of acoustic and electrical noises. Taking into account the delay in the transducer and the time shift, calculated by the correlation method and amounting to 34 and 51 μs at a frequency of 50 and 120 kHz, respectively, the wave propagation velocity was calculated for a known fixed base of 1000 mm.

Results and Discussion

The final result was the dependence of the propagation velocity of the antisymmetric Lamb wave mode on the angle of deviation of the path of wave propagation from pipe

generatrix (deviation angle), i.e. 0 degrees – direction along the pipe, along the generatrix, 90 degrees – circumferential direction of the pipe, along the envelope (figure 5).

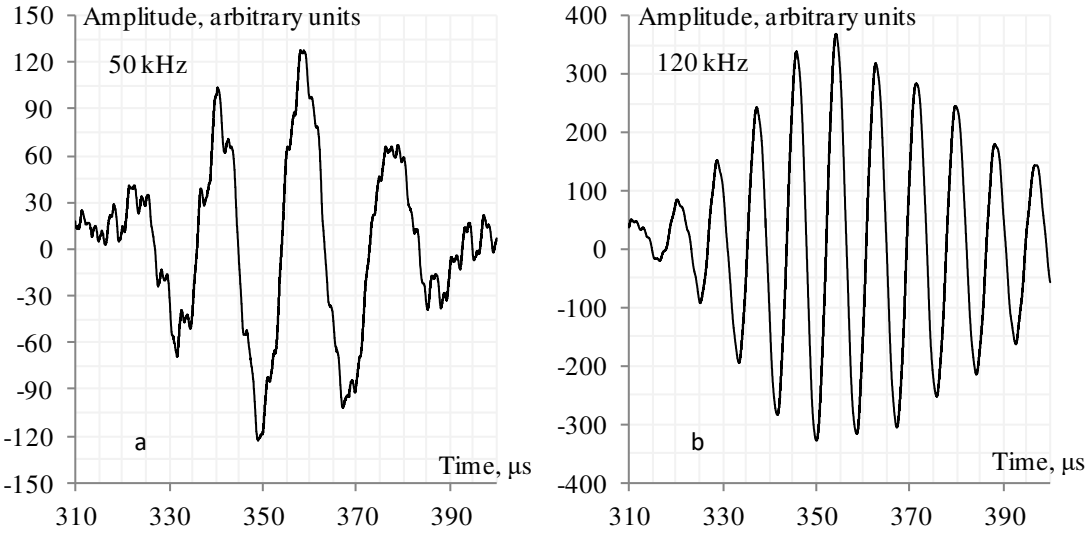

Figure 4. The received signal recorded by flaw detector at frequency of 50 kHz (a) and 120 kHz (b)

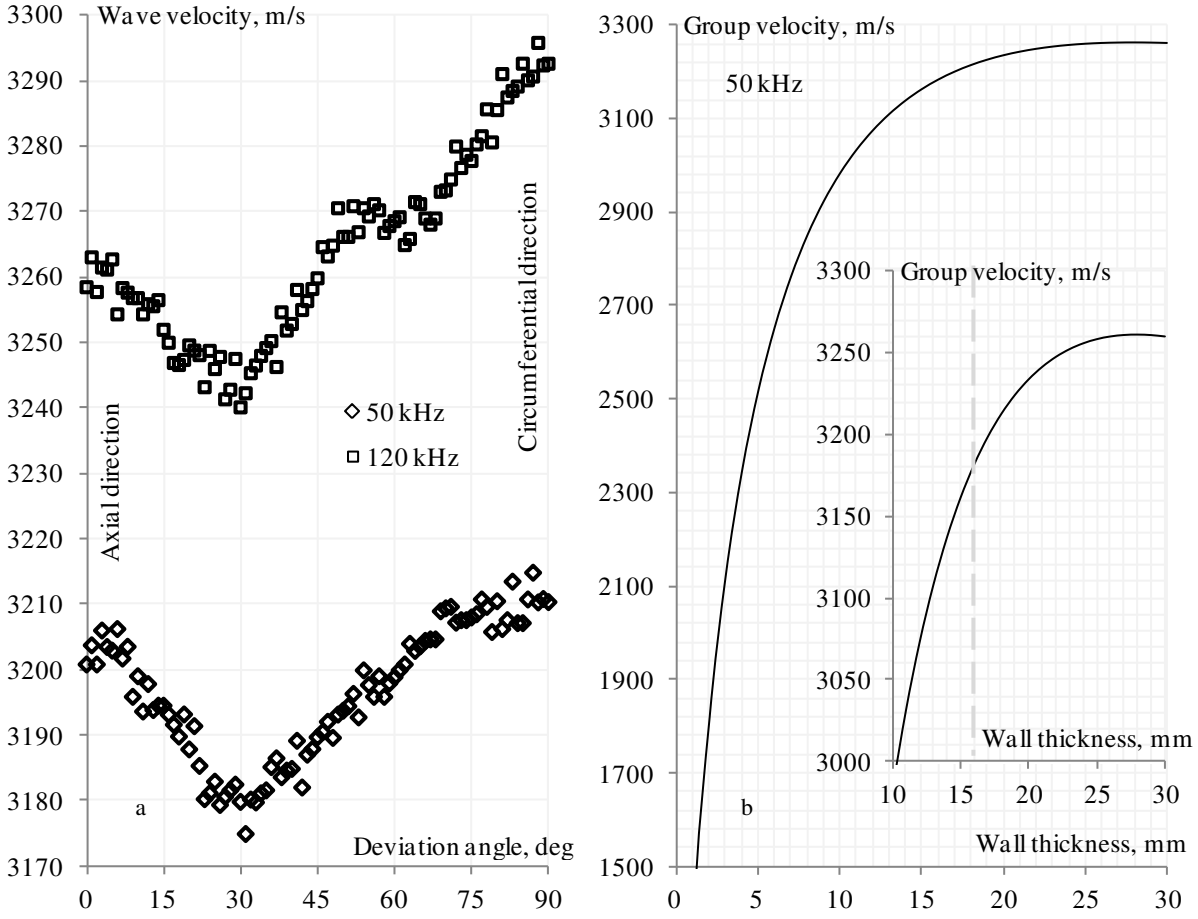

Figure 5. Dependence of antisymmetric Lamb wave mode on direction of the propagation in the hollow steel cylinder (a) and dependence of group velocity of antisymmetric Lamb wave mode on wall thickness in a steel plate at frequency of 50 kHz (b): deviation angle – angle of deviation of the path of wave propagation from pipe generatrix

The obtained dependence (figure 5a) shows two extrema: a maximum at an angle of 90 degrees and a minimum at an angle of 30 degrees. These extrema are explained by the simultaneous influence of the anisotropy of the pipe material properties and the geometric anisotropy (figure 6). The appearance of the maximum (figure 6b) is primarily explained by the presence of geometric anisotropy, as described in [49, 51], and its displacement relative to the pipe envelope (90 degrees) is associated with the anisotropy of the material properties (figure 6c). This shift will be the greater, the greater the anisotropy of the material properties (figure 6a). Also, the maximum and minimum are additionally shifted relative to the directions along the envelope (90 degrees) and along generatrix (0 degrees) of the pipe, respectively, due to the orientation of the sheet with pronounced anisotropy properties in the spiral welded pipe (figure 6d).

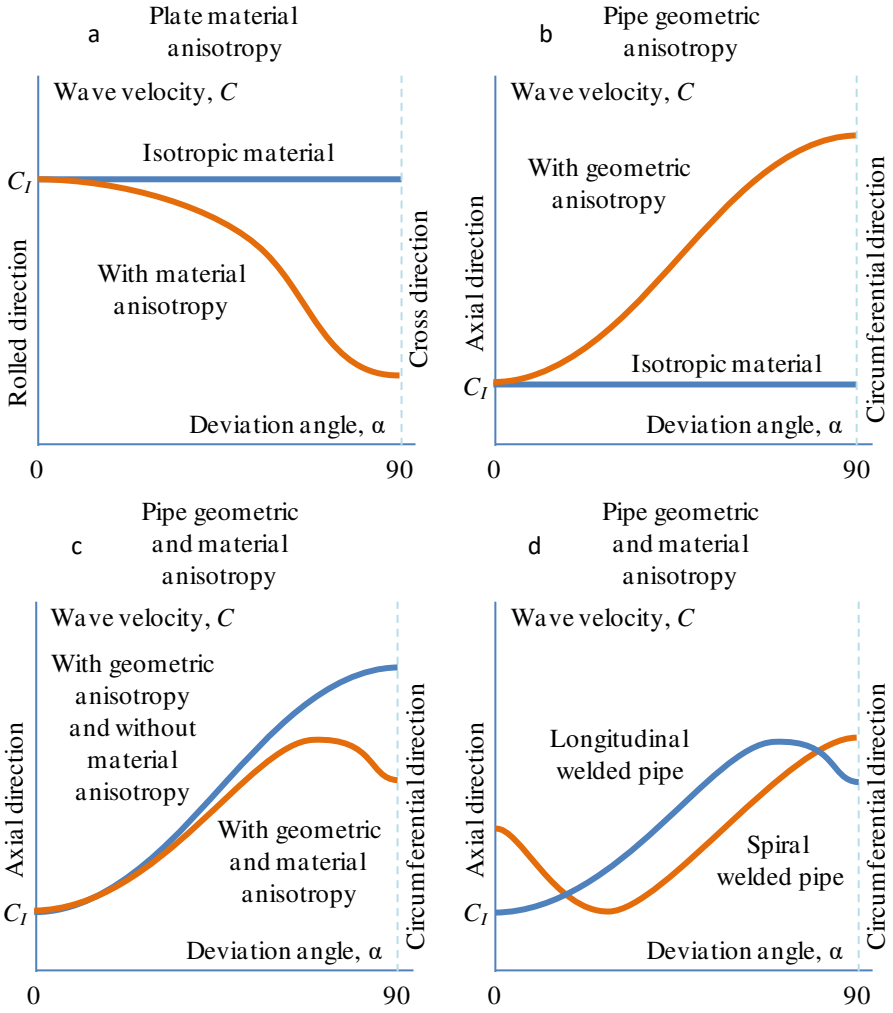

Figure 6. Schematic explanation of the formation of the shape of the dependence of the wave velocity on the deviation angle (degrees) in a spiral welded pipe: (a) influence of anisotropy of material properties, (b) influence of geometric anisotropy, (c) influence of anisotropy of material properties and geometric anisotropy, (d) influence of anisotropy of material properties and geometric anisotropy in spiral welded pipe, C_I – theoretical value of the wave velocity in isotropic material

Since the dispersion of the velocity of the antisymmetric Lamb wave mode is more pronounced at low frequencies, the qualitative dependences of the velocity at frequencies of 50 and 120 kHz have different forms. Velocities values change within range from 3240 m/s to

3295 m/s with 55 m/s range span at 120 kHz and 3180 m/s to 3215 m/s with 35 m/s range span at 50 kHz. In this case, at a frequency of 120 kHz, a "step" is observed in the range of angles from 50 to 65 degrees, caused by the presence of modes of a higher order.

Since geometric anisotropy has the same effect on the wave velocity at any frequency [50, 51], changes in the velocity range are associated with the anisotropy of the material properties and, to the greatest extent, with the velocity dispersion, caused by the influence of the pipe geometry. In this case, the more pronounced the velocity dispersion, the greater the influence on the change in the wave velocity is exerted by the pipe geometry. Thus, at a frequency of 50 kHz, when the pipe wall thickness changes from 16 mm to 1 mm, the velocity of the antisymmetric Lamb wave mode will change by 20 m/s, and at a wall thickness of 28 mm, the velocity will not change, i.e. the wave will not be sensitive to changes in the wall thickness with the given testing parameters.

CONCLUSIONS

Thus, based on the results of studies of the propagation of the antisymmetric Lamb wave mode in a hollow cylinder, the following conclusions can be drawn:

• qualitatively, the dependence of the velocity of the antisymmetric Lamb wave mode on the angle of deviation of the path of wave propagation from pipe generatrix is similar to the dependence of the horizontally polarized shear;

• to separate the types of waves during their excitation and reception, it is necessary to take into account the diagram of displacements in the wave at the given frequency;

• the limits of changing the velocity range at frequencies of 50 kHz and 120 kHz for a pipe with a diameter of 1020 mm and a wall thickness of 16 mm are 35 m/s and 55 m/s, respectively;

• the more pronounced the velocity dispersion, the more sensitive the wave to the pipe geometry;

• anisotropy of material properties is additionally superimposed on geometric anisotropy, which is expressed in displacements of extrema in the dependences of velocity on the angle of deviation of the path of wave propagation from pipe generatrix.

The research results can be used to improve the methods of guided wave testing, develop piezoelectric transducers with dry point contact and testing systems for flaw detection, thickness measurement and structural health monitoring of pipelines and their products.

ACKNOWLEDGEMENTS

This work was supported by the Russian Science Foundation (Project No. 18-79-10122).

REFERENCES

1. Buldakova, I. V., Volkova, L. V., & Muravyev, V. V. (2020). Stress distribution in pipe samples of gas pipelines with welded joints. *Intellektual'nye sistemy v proizvodstve [Intelligent Systems in Manufacturing], 18*(1), 4-8. doi: 10.22213/2410-9304-2020-1-4-8. (in Russian).
2. Murav'ev, V. V., Yakimov, A. V., Volkova, L. V., & Platunov, A. V. (2019). Investigation of biaxial stress state in R65 rails by acoustoelasticity method. *Intellektual'nye sistemy v proizvodstve [Intelligent Systems in Manufacturing], 17*(1), 19-25. doi: 10.22213/2410-9304-2019-1-19-25. (in Russian).

3. Budrin, A. Y. (2020). The influence of heat treatment on the propagation velocity of shear waves in steel bars. *Intellektual'nye sistemy v proizvodstve [Intelligent Systems in Manufacturing], 17*(4), 12-17. doi: 10.22213/2410-9304-2019-4-12-17. (in Russian).
4. Ida, N., & Meyendorf, N. (Eds.). (2019). *Handbook of advanced non-destructive evaluation.* Cham, Switzerland : Springer. ISBN 978-3-319-26553-7. doi: 10.1007/978-3-319-30050-4.
5. Uglov, A. L., Hlybov, A. A., Bychkov, A. L., & Kuvshinov, M. O. (2019). About non-destructive control of residual stresses in axisymmetric parts made of steel 03Ni17Co10W10MoTi. *Bulletin of Kalashnikov ISTU, 22*(4), 3-9. doi: 10.22213/2413-1172-2019-4-3-9. (in Russian).
6. Volkova, L. V., & Platunov, A. V. (2019). Rail base point inspection using the mirror through transmission testing technique on multiple reflections. *Bulletin of Kalashnikov ISTU, 22*(4), 38-45. doi: 10.22213/2413-1172-2019-4-38-45. (in Russian).
7. Milovzorov, G. V., Ilyin, A. P., & Red'kina, T. A. (2019). Methods for diagnosis of downhole pumping equipment condition based on dynamometry. *Bulletin of Kalashnikov ISTU, 22*(4), 64-72. doi: 10.22213/2413-1172-2019-4-64-72. (in Russian).
8. Uglov, A. L., Khlybov, A. A., Kolesnikov, M. V., Bystrukova, T. V., & Bychkov, A. L. (2019). On ultrasonic control of the thickness of plasma surfacing of copper-nickel alloy on a steel cylindrical surface. *Bulletin of Kalashnikov ISTU, 22*(3), 3-10. doi: 10.22213/2413-1172-2019-3-3-10. (in Russian).
9. Syas'ko, V. A., Golubev, S. S., & Ivkin, A. E. (2019). Experience of developing instruments for measuring firearm functional coating thickness. *Bulletin of Kalashnikov ISTU, 22*(3), 11-18. doi: 10.22213/2413-1172-2019-3-11-18. (in Russian).
10. Zlobin, D. V., & Muravieva, O. V. (2012). Development features of electromagnetic acoustic defectoscopy equipment for bar iron using rod waves. *Bulletin of Kalashnikov ISTU,* (4), 099-104. ISSN 2413-1172. (in Russian).
11. Strizhak, V. A., Hasanov, R. R., & Pryakhin, A. V. (2018). Features of excitation of an electromagnetic acoustic transducer under a waveguide method of testing. *Bulletin of Kalashnikov ISTU, 21*(2), 159-166. doi: 10.22213/2413-1172-2018-2-159-166. (in Russian).
12. Muravyova, O. V., & Murashov, S. A. (2011). Use of torsional waves for detection of operational defects in pump rods and tubing. *Bulletin of Kalashnikov ISTU,* (2), 149-154. ISSN 2413-1172. (in Russian).
13. Strizhak, V. A., Pryakhin, A. V., Khasanov, R. R., & Mkrtchyan, S. S. (2019). Flaw detection of composite rebar by acoustic wave guided technique. *Bulletin of Kalashnikov ISTU, 22*(1), 78-88. doi: 10.22213/2413-1172-2019-1-78-88. (in Russian).
14. Strizhak, V. A., Hasanov, R. R., & Pryakhin, A. V. (2018). Features of excitation of an electromagnetic acoustic transducer under a waveguide method of testing. *Bulletin of Kalashnikov ISTU, 21*(2), 159-166. doi: 10.22213/2413-1172-2018-2-159-166. (in Russian).
15. Jenot, F., Ouaftouh, M., Duquennoy, M., & Ourak, M. (2001). Corrosion thickness gauging in plates using Lamb wave group velocity measurements. *Measurement Science and Technology, 12*(8), 1287-1293. doi: 10.1088/0957-0233/12/8/341.

16. Lowe, M. J. S., Cawley, P., Kao, J. Y., & Diligent, O. (2000, May). Prediction and measurement of the reflection of the fundamental anti-symmetric Lamb wave from cracks and notches. *AIP Conference Proceedings, 509*(1), 193-200. doi: 10.1063/1.1306051.
17. Lowe, M. J., Cawley, P., Kao, J. Y., & Diligent, O. (2002). The low frequency reflection characteristics of the fundamental antisymmetric Lamb wave a0 from a rectangular notch in a plate. *The Journal of the Acoustical Society of America, 112*(6), 2612-2622. doi: 10.1121/1.1512702.
18. Lu, Y., Ye, L., Su, Z., & Yang, C. (2008). Quantitative assessment of through-thickness crack size based on Lamb wave scattering in aluminium plates. *NDT & E International, 41*(1), 59-68. doi: 10.1016/j.ndteint.2007.07.003.
19. Park, M. H., Kim, I. S., & Yoon, Y. K. (1996). Ultrasonic inspection of long steel pipes using Lamb waves. *NDT & E International, 29*(1), 13-20. doi: 10.1016/0963-8695(95)00030-5.
20. Ramadas, C., Janardhan Padiyar, M., Balasubramaniam, K., Joshi, M., & Krishnamurthy, C. V. (2010). Delamination size detection using time of flight of anti-symmetric (A_o) and mode converted A_o mode of guided Lamb waves. *Journal of Intelligent Material Systems and Structures, 21*(8), 817-825. doi: 10.1177/1045389X10367836.
21. Giurgiutiu, V. (2005). Tuned Lamb wave excitation and detection with piezoelectric wafer active sensors for structural health monitoring. *Journal of Intelligent Material Systems and Structures, 16*(4), 291-305. doi: 10.1177/1045389X05050106.
22. Azizi, N., Saadatpour, M. M., & Mahzoon, M. (2019). Analyzing first symmetric and antisymmetric Lamb wave modes in functionally graded thick plates by using spectral plate elements. *International Journal of Mechanical Sciences, 150*, 484-494. doi: 10.1016/
j.ijmecsci.2018.10.030.
23. Lasn, K., Klauson, A., Chati, F., & Décultot, D. (2011). Experimental determination of elastic constants of an orthotropic composite plate by using lamb waves. *Mechanics of Composite Materials, 47*(4), 435. doi: 10.1007/s11029-011-9221-y.
24. Nenadic, I. Z., Urban, M. W., Mitchell, S. A., & Greenleaf, J. F. (2011). Lamb wave dispersion ultrasound vibrometry (LDUV) method for quantifying mechanical properties of viscoelastic solids. *Physics in Medicine & Biology, 56*(7), 2245-2264. doi: 10.1088/0031-9155/56/7/021.
25. Leonard, K. R., Malyarenko, E. V., & Hinders, M. K. (2002). Ultrasonic Lamb wave tomography. *Inverse problems, 18*(6), 1795-1808. doi: 10.1088/0266-5611/18/6/322.
26. Zhao, X., Royer, R. L., Owens, S. E., & Rose, J. L. (2011). Ultrasonic Lamb wave tomography in structural health monitoring. *Smart Materials and Structures, 20*(10), 105002. doi: 10.1088/0964-1726/20/10/105002.
27. Ho, K. S., Billson, D. R., & Hutchins, D. A. (2007). Ultrasonic Lamb wave tomography using scanned EMATs and wavelet processing. *Nondestructive Testing and Evaluation, 22*(1), 19-34. doi: 10.1080/10589750701327890.
28. Pei, J., Yousuf, M. I., Degertekin, F. L., Honein, B. V., & Khuri-Yakub, B. T. (1996). Lamb wave tomography and its application in pipe erosion/corrosion monitoring. *Journal of Research in Nondestructive Evaluation, 8*(4), 189-197. doi: 10.1007/BF02433949.

29. Leonard, K. R., & Hinders, M. K. (2003). Guided wave helical ultrasonic tomography of pipes. *The Journal of the Acoustical Society of America, 114*(2), 767-774. doi: 10.1121/1.1593068.

30. Wang, L., & Yuan, F. G. (2007). Group velocity and characteristic wave curves of Lamb waves in composites: Modeling and experiments. *Composites Science and Technology, 67*(7-8), 1370-1384. doi: 10.1016/j.compscitech.2006.09.023.

31. Veidt, M., & Ng, C. T. (2011). Influence of stacking sequence on scattering characteristics of the fundamental anti-symmetric Lamb wave at through holes in composite laminates. *The Journal of the Acoustical Society of America, 129*(3), 1280-1287. doi: 10.1121/1.3533742.

32. Kim, Y. H., Kim, D. H., Han, J. H., & Kim, C. G. (2007). Damage assessment in layered composites using spectral analysis and Lamb wave. *Composites Part B: Engineering, 38*(7-8), 800-809. doi: 10.1016/j.compositesb.2006.12.010.

33. Bingham, J., & Hinders, M. (2009). Lamb wave detection of delaminations in large diameter pipe coatings. *The Open Acoustics Journal, 2*(1), 75-86. doi: 10.2174/1874837600902010075.

34. Soleimanpour, R., & Ng, C. T. (2016). Scattering of the fundamental anti-symmetric Lamb wave at through-thickness notches in isotropic plates. *Journal of Civil Structural Health Monitoring, 6*(3), 447-459. doi: 10.1007/s13349-016-0166-7.

35. Ng, Ching-Tai. (2015). On accuracy of analytical modeling of Lamb wave scattering at delaminations in multilayered isotropic plates. *International Journal of Structural Stability and Dynamics, 15*(8), 1540010. doi: 10.1142/S0219455415400106.

36. Chen, J., Su, Z., & Cheng, L. (2009). Identification of corrosion damage in submerged structures using fundamental anti-symmetric Lamb waves. *Smart Materials and Structures, 19*(1), 015004. doi: 10.1088/0964-1726/19/1/015004.

37. Ahmad, Z. A. B., Vivar-Perez, J. M., & Gabbert, U. (2013). Semi-analytical finite element method for modeling of Lamb wave propagation. *CEAS Aeronautical Journal, 4*(1), 21-33. doi: 10.1007/s13272-012-0056-6.

38. Hayward, G., & Hyslop, J. (2006). Determination of Lamb wave dispersion data in lossy anisotropic plates using time domain finite element analysis. Part I: theory and experimental verification. *IEEE Transactions on Ultrasonics, Ferroelectrics, and Frequency Control, 53*(2), 443-448. doi: 10.1109/TUFFC.2006.1593383.

39. Ramadas, C., Balasubramaniam, K., Joshi, M., & Krishnamurthy, C. V. (2009). Interaction of the primary anti-symmetric Lamb mode (A_o) with symmetric delaminations: numerical and experimental studies. *Smart Materials and Structures, 18*(8), 085011. doi: 10.1088/0964-1726/18/8/085011.

40. Srivastava, A., & di Scalea, F. L. (2009). On the existence of antisymmetric or symmetric Lamb waves at nonlinear higher harmonics. *Journal of Sound and Vibration, 323*(3-5), 932-943. doi: 10.1016/j.jsv.2009.01.027.

41. Wu, X. H., Shen, Y. P., & Sun, Q. (2007). Lamb wave propagation in magnetoelectroelastic plates. *Applied Acoustics, 68*(10), 1224-1240. doi: 10.1016/j.apacoust.2006.07.013.

42. Tua, P. S., Quek, S. T., & Wang, Q. (2005). Detection of cracks in cylindrical pipes and plates using piezo-actuated Lamb waves. *Smart Materials and Structures, 14*(6), 1325-1342. doi: 10.1088/0964-1726/14/6/025.

43. Lee, J. K., & Kim, Y. Y. (2016). Tuned double-coil EMATs for omnidirectional symmetric mode Lamb wave generation. *NDT & E International, 83*, 38-47. doi: 10.1016/j.ndteint.2016.06.001.

44. Sun, W., Liu, G., Xia, H., & Xia, Z. (2018). A modified design of the omnidirectional EMAT for antisymmetric Lamb wave generation. *Sensors and Actuators A: Physical, 282,* 251-258. doi: 10.1016/j.sna.2018.07.030.

45. Cheng, J. C., & Zhang, S. Y. (1999). Quantitative theory for laser-generated Lamb waves in orthotropic thin plates. *Applied Physics Letters, 74*(14), 2087-2089. doi: 10.1063/1.123766.

46. Nakano, H., & Nagai, S. (1991). Laser generation of antisymmetric Lamb waves in thin plates. *Ultrasonics, 29*(3), 230-234. doi: 10.1016/0041-624X(91)90061-C.

47. Kazys, R. J., Vilpisauskas, A., & Sestoke, J. (2018). Application of air-coupled ultrasonic arrays for excitation of a slow antisymmetric Lamb wave. *Sensors, 18*(8), 2636. doi: 10.3390/s18082636.

48. Fan, Z., Jiang, W., & Wright, W. M. (2018). Non-contact ultrasonic gas flow metering using air-coupled leaky Lamb waves. *Ultrasonics, 89*, 74-83. doi: 10.1016/j.ultras.2018.04.008.

49. Myshkin Yu. V., Murav'eva O. V., Sannikova Yu. O., & Chukhlanceva T. S. (2018) The propagation of horizontally polarized shear wave in the hollow cylinder. In *Instrumentation Engineering, Electronics and Telecommunications - 2018: Proceedings of the IV International Forum: 12-14 Dec. 2018* (pp. 51-65). Izhevsk, Russia : Publ. House of Kalashnikov ISTU. doi: 10.22213/2658-3658-2018-51-65.

50. Myshkin, Y. V., Murav'eva, O. V., Fotina, A. A., & Chukhlanceva, T. S. (2019). The propagation of symmetric Lamb wave in the hollow cylinder. In *Instrumentation Engineering, Electronics and Telecommunications - 2019: Proceedings of the V International Forum 20-22 Nov. 2019* (pp. 85-97). Izhevsk, Russia : Publ. House of Kalashnikov ISTU. doi: 10.22213/2658-3658-2019-85-97.

51. Myshkin, Y. V., Muravieva, O. V., Voronchikhin, S. Y., Samokrutov, A. A., & Shevaldykin, V. G. (2019). Geometric anisotropy of velocity of horizontally polarized shear wave in pipe. *Journal of Physics: Conference Series, 1327*(1), 012023. doi: 10.1088/1742-6596/1327/1/012023.

DOI: 10.22213/2658-3658-2020-24-31

Diagnostics of Robot Drives Based on DC Motors by Identifiability Criterion of Nonlinear Discrete Model in State Space

Yu. R. Nikitin, S. A. Trefilov

Department of Mechatronic Systems,
Kalashnikov Izhevsk State Technical University, Izhevsk, Russian Federation
E-mail: nikitin@istu.ru

Received: June 15, 2020

Abstract. The paper studies robot drives by the identifiability criterion based on a discrete digital control model. Criteria of observability, controllability and identifiability of drives as a function of the rank of an extended state matrix with a measurement matrix are considered, in which the relative errors of the information-measuring system are analytically taken into account. An algorithm is proposed for calculating the identifiability criterion for a nonlinear control system in a discrete linearization version. It is proposed to use identification in terms of the correspondence of the mathematical model to the results of the operation of the object. At each step, the determinant of the extended matrix is calculated, which is compared with a constant that numerically divides the space of the state matrices. Thus, the operation of the drives itself makes it possible to determine its identifiability. As a criterion for the optimality of the identification algorithm, a decision-making optimality criterion is chosen in combination with an identifiability criterion for an optimal control algorithm by the criterion of minimum quadratic form. The vector-matrix model of drives in the state space is presented taking into account the relative accuracy of measuring the state of the information-measuring subsystem of drives. It is proposed for practical problems to determine the identifiability criterion by modeling the state matrix for cases when the state matrix parameters exit the space of realizable parameters of serviceable drives. The research results obtained can be used to build diagnostic systems for robot drives.

Keywords: Diagnostics, Identification, State space, Velocity control, DC motors, Robots, Modeling

INTRODUCTION

To ensure high reliability of robot drives, an effective diagnostic system is required. For the diagnosis of robot drives, an algorithm is proposed for deciding on their identifiability based on a discrete nonlinear control model in the state space.

The method of identification in the state space has been actively developed over the past two decades and has been successfully implemented in many industries. One of the first P. Eickhoff performed the theoretical justification of identification, developed algorithms and methods of identification [1, 2]. The identification of dynamical systems is devoted to the work of the following authors: D. Gropp [3], L. Ljung [4], E. P. Sage and J. L. Melsa [5, 6],

and among Russian authors - Ya. Z. Tsypkina [7], N. S. Reibman [8], Sh. E. Steinberg [9] and others.

R. Beard developed an observer-based defect detection scheme [10]. Jones continued these studies and developed the Beard-Jones Fault Detection Filter [11]. In the 1980s and early 1990s, the main approaches to quantitative diagnostics were developed: an observer-based approach, a parameter estimation method, etc. Some important works in this direction are Frank [12], Isermann [13], and Basville and Nikiforov [14]. The developed methods are well theoretically justified and are classic diagnostic methods. These techniques are based on analytical redundancy, which is a model that describes the diagnosed technical system. On diagnostics of robot drives, articles and monographs have been published [15-26], where approaches are considered both on the basis of the parametric approach and on the basis of continuous and discrete models of drives in the state space.

RESEARCH PROBLEM STATEMENT

For robot drives based on a DC motors, which are widely used in robot drives, control equations for continuous nonlinear systems in the state space are given

$$\dot{\mathbf{x}} = \mathbf{A}\mathbf{x} + \mathbf{B}\mathbf{u}, \tag{1}$$

$$\mathbf{y} = \mathbf{C}\mathbf{x}, \tag{2}$$

where $\mathbf{A}$ is the state matrix, $\mathbf{B}$ is the control matrix, $\mathbf{C}$ is the measurement matrix, $\mathbf{x}$ is the state vector.

The classical model of a DC motor with constant parameters does not correspond to reality in the entire operating range. Therefore, nonlinearity associated with viscous friction was added.

The following differential equations of the first order are known for the robot drives model based on a DC motors:

$$U = R\left(T\frac{dI}{dt} + I\right) + e, \tag{3}$$

$$J\frac{d\omega}{dt} = M - k_{fr}\omega - M_L, \tag{4}$$

$$\omega = \frac{d\theta}{dt}, \tag{5}$$

$$e = k_E\omega, \quad M = k_M I, \tag{6}$$

$$T = \frac{L}{R}, \tag{7}$$

where U, I, e are the voltage, current and counter-EMF of the DC motor anchor; L, R, T are inductance, resistance and electromagnetic time constant of the anchor DC motor; ω, M, M_L, θ are angular velocity, electromagnetic moment of the DC motor, the load moment and the angle of a rotation of the DC motor shaft; J is moment of inertia of the rotor DC motor and load; k_E, k_M are coefficients that are structural constants of the engine; k_{fr} is coefficient of viscous friction of the DC motor.

Further, equation (3) for continuous nonlinear systems is written in the form of Cauchy:

$$L\frac{dI}{dt} = -RI - k_E\omega + U. \tag{8}$$

To identify the DC motor model, a pair of equations (8) and (4) is used in the state space on the basis of which the vector-matrix model is built. The scalar value, the supply voltage of the drive *U*, is specified as the control vector.

In general terms, when at least one of the matrixes **A**, **B**, **C** are time-dependent, the task is non-linear and has only particular solutions.

To find the equation in the state space, we represent equations (1, 2) in a discrete form, and the sampling time *T* tends to zero, and the trajectory of motion in each discrete section is linear.

We write the solution for the nonlinear problem in a discrete form, when the matrix **A**, **B**, **C** are constant at time instants *k, k* = 0, 1, 2, 3, … :

$$\frac{\mathbf{x}_{k+1} - \mathbf{x}_k}{T} = \mathbf{A}_k\mathbf{x}_k + \mathbf{B}_k\mathbf{u}_k, \tag{9}$$

or

$$\mathbf{x}_{k+1} = \tilde{\mathbf{A}}_k\mathbf{x}_k + \tilde{\mathbf{B}}_k\mathbf{u}_k, \tag{10}$$

where $\tilde{\mathbf{A}}_k = T\mathbf{A} + \mathbf{E}$, $\tilde{\mathbf{B}}_k = T\mathbf{B}_k$.

This equation (10) relates the transition of the system from state $\mathbf{x}_k$ to state $\mathbf{x}_{k+1}$. On the segment *T*, we take the values of the matrices $\mathbf{A}_k$, $\mathbf{B}_k$ and $\mathbf{C}_k$ as constants. For convenience, in the following entries we remove the "wavy line" sign.

We assume that the matrix $\mathbf{C}^{-1} = \mathbf{C}_k^{-1}$ at each step *k* does not change, is determined by the information-measuring system, can be represented as

$$\mathbf{C}^{-1} = \mathbf{E} + \boldsymbol{\xi}_n, \tag{11}$$

where $\boldsymbol{\xi}_n = \begin{bmatrix}\xi_1 & \xi_2 & \dots & \xi_n\end{bmatrix}^{\mathrm{T}}$ is a random vector representing the random nature of the measurements by the information-measuring system that is part of the drives.

ROBOT DRIVE MODEL IDENTIFICATION

Consider the question of identifying the model of robot drives from the point of view of the analysis of expression (10), where at each linearization step the rank of the expanded matrix is the criterion of identifiability and observability.

$$\min\det\left[\mathbf{C}_k^T \vdots \mathbf{A}_k^T\mathbf{C}_k^T\right] \geq \gamma, \tag{12}$$

where $\mathbf{C}_k^T$ is the transported measurement matrix, taking into account the accuracy class of the sensors; γ is the threshold value of the determinants determined by the identification object and close to zero.

Considering that in many practical control tasks the dimensions of the tasks do not exceed ten, and the relative measurement accuracy is equal to units of percent, we can conclude that only the state matrix affects the identifiability of the robot drive model

$$\mathbf{A}_k^{\mathrm{T}},\ k = \overline{1,n}. \tag{13}$$

This matrix will ultimately determine the rank of matrix (12).

It is proposed for practical tasks to determine the identifiability of the drive model in the form

$$\min \det \mathbf{A}_k^{\mathrm{T}} \det \mathbf{C}_k^T \geq \gamma. \tag{14}$$

DIAGNOSTICS OF ROBOT DRIVES BASED ON A DC MOTOR ACCORDING TO THE IDENTIFIABILITY CRITERION OF A DRIVE MODEL

Consider the diagnosis of drives based on the DC motor in the state space. Since the drive regulator must provide control over the moment and speed of rotation, the armature current I and the armature speed ω are chosen as generalized coordinates. The control is the voltage at the armature U, the disturbance is the load resistance moment M_L. The model parameters are the active resistance and inductance of the circuit and the armature, denoted respectively by R, and L, as well as the reduced moment of inertia J and the design constants k_E and k_M. By resolving the original system with respect to the first derivatives, the DC motor equation in the state space is obtained.

We write the vector-matrix model of the DC motor in the form (1, 2) in the state space. The novelty of the DC motor model is that the expected torque M is taken into account based on a given trajectory of movement.

$$\dot{\mathbf{x}} = \begin{bmatrix} \dot{I} \\ \dot{\omega} \end{bmatrix} = \begin{bmatrix} -\frac{R}{L} & -\frac{k_E}{L} \\ \frac{k_M}{J} & -\frac{k_{fr}\omega + M}{J\omega} \end{bmatrix} \begin{bmatrix} I \\ \omega \end{bmatrix} + \begin{bmatrix} \frac{1}{L} \\ 0 \end{bmatrix} \mathbf{u}, \tag{15}$$

$$\mathbf{y} = \begin{bmatrix} I \\ \omega \end{bmatrix} = \begin{bmatrix} 1 & 0 \\ 0 & 1 \end{bmatrix} \mathbf{x}, , \tag{16}$$

We write the vector-matrix model of a DC motor in the form (10).

$$\mathbf{x}(k+1) = \begin{bmatrix} 1 - T\frac{R}{L} & -T\frac{k_E}{L} \\ T\frac{k_M}{J} & 1 - T\frac{k_{fr}\omega + M_L(k)}{J\omega(k)} \end{bmatrix} \times \begin{bmatrix} I(k) \\ \omega(k) \end{bmatrix} + \begin{bmatrix} \frac{1}{L} \\ 0 \end{bmatrix} \mathbf{u}(k), \tag{17}$$

$$\mathbf{y}(k) = \begin{bmatrix} \hat{I}(k) \\ \hat{\omega}(k) \end{bmatrix} = \begin{bmatrix} 1 + h\xi & 0 \\ 0 & 1 + h\xi \end{bmatrix} \mathbf{x}(k), \tag{18}$$

where $M_L(k) = (\omega(k+1) - \hat{\omega}(k))\frac{J}{T}$; $\hat{I}(k)$, $\hat{\omega}(k)$ are measured value of current and angular velocity; $\omega(k+1)$ is the planned value of the angular velocity.

We calculate the load moment in the determinant of matrix **A** for equality

$$\det \mathbf{A} = \begin{bmatrix} 1 - T\frac{R}{L} & -T\frac{k_E}{L} \\ T\frac{k_M}{J} & 1 - T\frac{k_{fr\_mp}\omega + M_L(k)}{J\omega(k)} \end{bmatrix} = 0. \tag{19}$$

The fact that matrix **A** is equal to zero leads (14) to the non-identifiability of the robot drive model in the state space.

The expression $M(k) = (\omega(k+1) - \hat{\omega}(k))J / T$ gives the relationship between the mechanical parameters of the DC motor, allows you to determine the interval of change of values without loss of identifiability. In addition, restrictions on the maximum rotation speed, electric current, and voltage for this drive must be considered.

COMPUTATIONAL EXPERIMENTS TO STUDY THE IDENTIFIABILITY OF THE DC MOTOR MODEL IN DISCRETE FORM

The scheme of the DC motor model for calculating the determinant of the state matrix **A** was built in the software SimInTech "Environment for Dynamic Modeling of Technical Systems", developed by 3V Service[1].

Figure 1 shows the model for calculating the determinant of the state matrix **A** and moment of the DC motor for various values of the armature winding resistance in the case of inter-turn faults in program SimInTech.

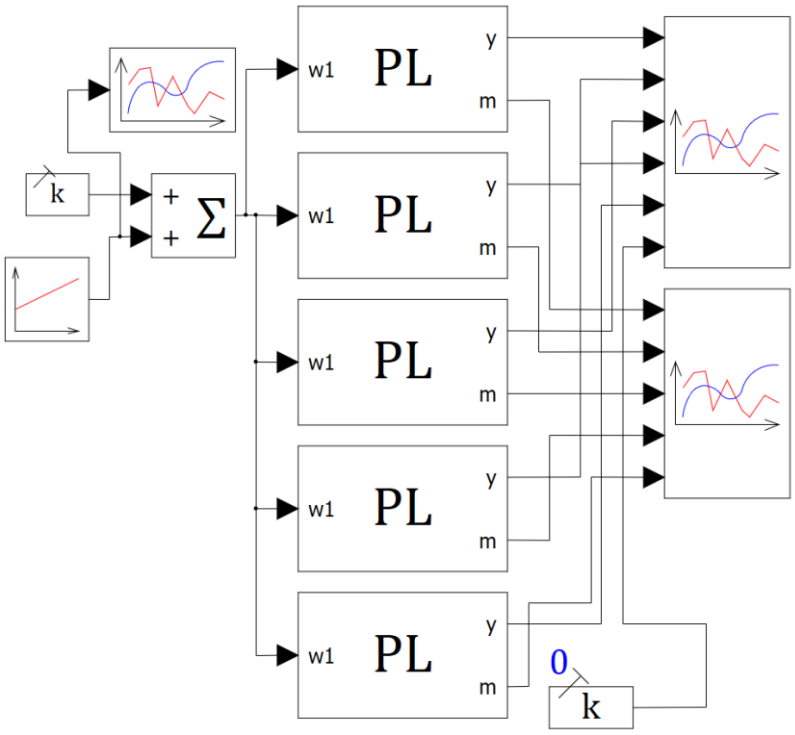

Figure 1. The model for calculating the determinant of the state matrix **A** and moment of the DC motor in program SimInTech

The gamma threshold was chosen 0.05. Figure 2 shows the dependence of the determinant of the state matrix **A** on the armature winding resistance R. The influence of changes in the resistance of the armature winding of the DC motor on the determinant of the state matrix **A** was studied. An analysis of the dependence of the determinant of the state matrix **A** on the resistance value of the armature of the DC motor armature shows that the allowable angular velocity decreases from 360 rad/s to 345 rad/s.

[1] Available at: http://simintech.ru/

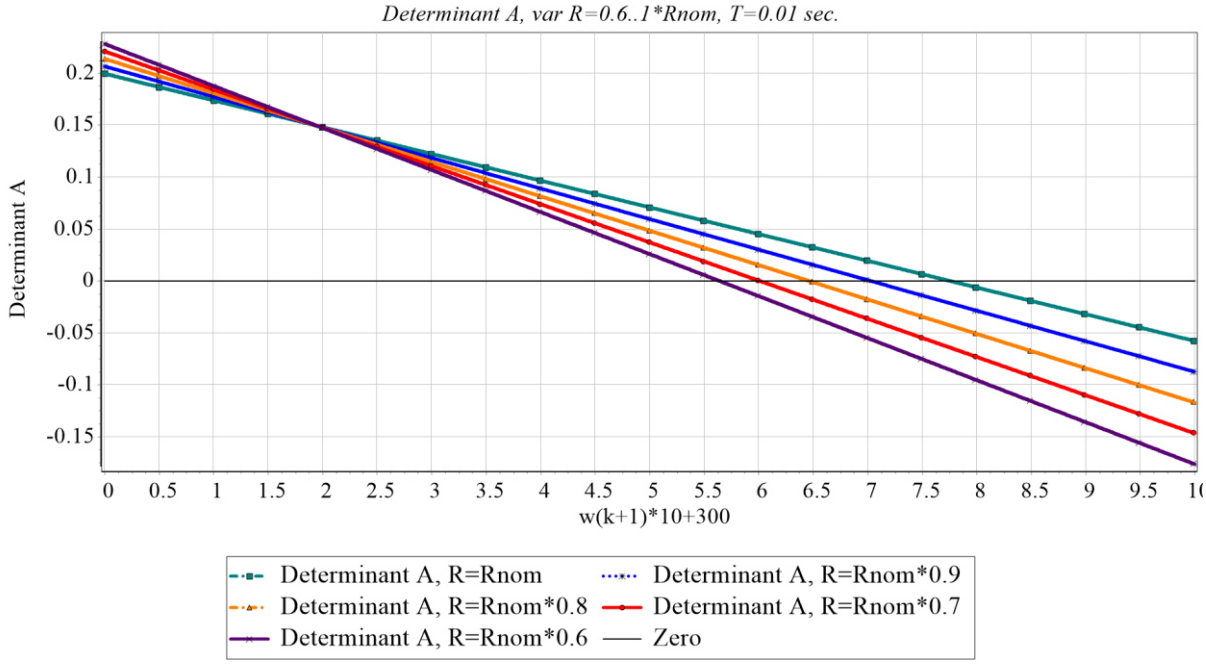

Figure 2. Dependence of the determinant of the state matrix **A** on the armature winding resistance R

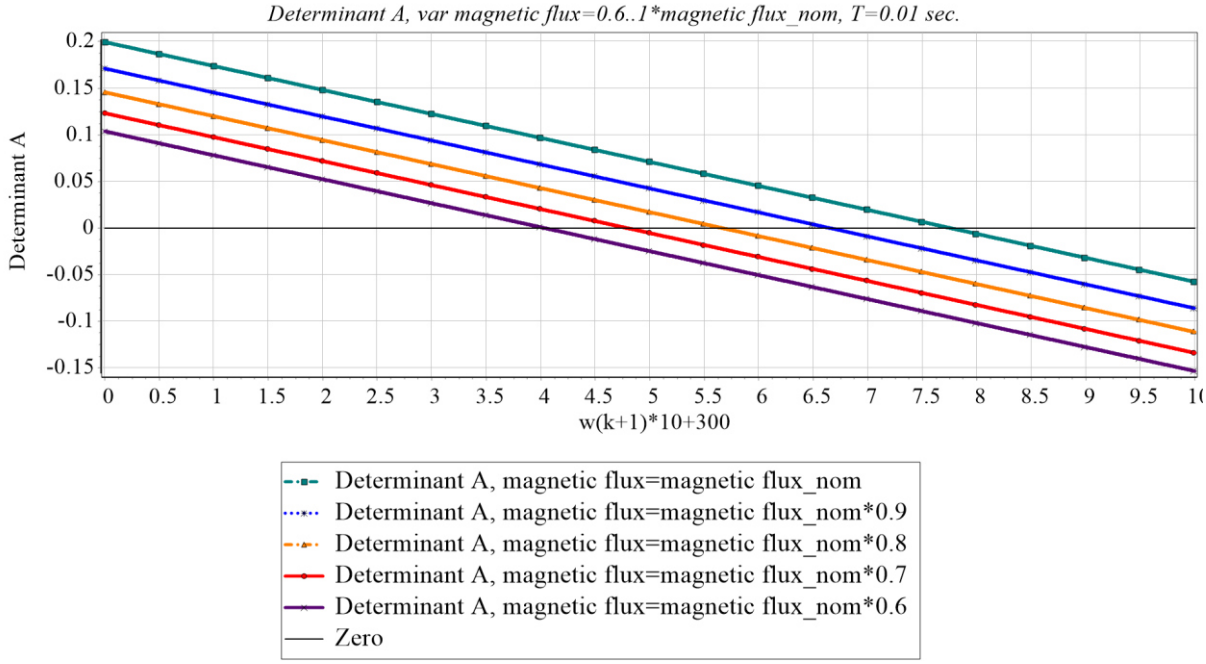

Figure 3. Dependence of the determinant of the state matrix **A** on the magnetic flux of the DC motor

CONCLUSION

Figure 3 shows the dependence of the determinant of the state matrix **A** on the magnetic flux of the DC motor. An analysis of the dependence of the determinant of the state matrix **A** on the magnetic flux of the DC motor shows that the allowable angular velocity decreases from 360 rad/s to 320 rad/s.

This paper presents an algorithm for identifying nonlinear complex objects based on a discrete digital control model. As a criterion for the optimality of the identification algo-

rithm, a decision-making criterion is selected in combination with an identifiability criterion for the control algorithm. Identification criteria, allowing either the degree of conformity of the models to the control object using the model of the measuring matrix or the combination of models of the state matrix and measuring matrix. The region of permissible values of angular velocities is obtained depending on the armature winding resistance and the magnetic flux of the DC motor.

The reported study was funded by RFBR according to the research project № 18-08-00772 A.

REFERENCES

1. Eykhoff, P. (1974). *System identification: parameter and state estimation.* New York : Wiley-Interscience, 555 pp.
2. Eykhoff, P. (Ed.). (1981). *Trends and progress in system identification.* Oxford, England: Pergamon, 402 pp.
3. Graupe, D. (1976). *Identification of system.* New York, USA : R.E.Krieger Publishing Company, 302 pp.
4. Ljung, L. (1997). *System identification: theory for the user* (2nd ed.). Pearson PTG, 640 pp.
5. Sage, A., & Melsa, J. (1971). *System identification.* New York, USA : Academic press, 221 pp.
6. Sage, A., & Melsa, J. (1971). *Estimation theory with applications to communications and control.* New York, USA : McGraw-Hill, 496 pp.
7. Cypkin, Ja. Z. (1984). *Osnovy informacionnoj teorii identifikacii [Fundamentals of identification information theory].* Moscow, Russia : Nauka, 320 pp. (in Russian).
8. Rajbman, N. S. (1970). *Chto takoe identifikacija? [What is identification?].* Moscow, Russia : Nauka, 118 pp. (in Russian).
9. Shtejnberg, Sh. E. (1987). *Identifikacija v sistemah upravlenija [Identification in control systems].* Moscow, Russia : Jenergoatomizdat, 80 pp. (in Russian).
10. Beard, R. V. (1971). *Failure accommodation in linear system through selfreorganization* (PhD thesis), MIT, USA, 376 pp.
11. Jones, H. L. (1973). *Failure detection in linear systems* (PhD thesis). MIT, USA, 459 pp.
12. Frank, P. M. (1990). Fault diagnosis in dynamic systems using analytical and knowledge-based redundancy: a survey and some new results. *Automatica, 26*(3), 459-474. doi: 10.1016/0005-1098(90)90018-D.
13. Isermann, R. (2006). *Fault-diagnosis systems: an introduction from fault detection to fault tolerance.* Berlin; New York : Springer, 475 pp.
14. Basseville, M., & Nikiforov, I. V. (1993). *Detection of abrupt changes: theory and application.* Prentice Hall information and system sciences series. Englewood Cliffs, New Jersey, USA : Prentice Hall, 447 pp.
15. Ding, S. X. (2008). *Model-based fault diagnosis techniques. Design schemes, algorithms, and tools.* Berlin, Heidelberg : Springer, 473 pp. doi: 10.1007/978-3-540-76304-8.
16. Costa, B. S. J. (2016). Fuzzy fault detection and diagnosis. In *Handbook on computational intelligence: Vol. 2. Fuzzy logic, systems, artifical neural networks, and learning systems.* World Scientific Publishing Co. Pte. Ltd., pp. 251-288.

17. Luo, H. (2017). Plug-and-play monitoring and performance optimization for industrial automation processes. Springer Vieweg, 158 pp. doi: 10.1007/978-3-658-15928-3.

18. Trefilov, S., & Nikitin, Y. (2018). Automatic warehouses with transport robots of increased reliability. *Acta Logistica, 5*(1), 19-23. doi: 10.22306/al.v5i1.86.

19. Zhirabok, A. N., Shumskii, A. E., Solyanik, S. P., & Suvorov, A. Yu. (2017). Design of nonlinear robust diagnostic observers. *Automation and Remote Control, 78*(9), 1572–1584. doi: 10.1134/S000511791709003X.

20. Zhirabok, A. N., & Shumsky, A. E. (2019). Nonparametric method for diagnosis of nonlinear dynamic systems. *Automation and Remote Control, 80*(2), 217–233. doi: 10.1134/S0005117919020024.

21. Zhirabok, A. N., Shumsky, A. E., Solyanik, S. P., & Suvorov, A. Yu. (2017). Design of nonlinear robust diagnostic observers. *Automation and Remote Control, 78*(9), 1572-1584. doi: 10.1134/S000511791709003X.

22. Stepanov, P. I., Lagutkin, S. V., & Nikitin, Yu. R. (2013). Kompleksnaja tokovaja i vibrodiagnostika jelektromehanicheskih sistem [Integrated current and vibration diagnostics of electromechanical systems]. *Intellektual'nye sistemy v proizvodstve [Intelligent Systems in Manufacturing],* (2), 160-165. (in Russian).

23. Stepanov, P. I., Lagutkin, S. V., & Nikitin, Yu. R. (2014). Mehanicheskie i jelektricheskie diagnosticheskie parametry jelektricheskih privodov [Mechanical and electrical diagnostic parameters of electric drives]. *Intellektual'nye sistemy v proizvodstve [Intelligent Systems in Manufacturing],* (2), 59-63. (in Russian).

24. Nikitin, Yu. R., Trefilov, S. A., Abramov, A. I., Abramov, I. V., Turygin, Yu. V., & Romanov, A. V. (2018). Diagnostirovanie privodov mobil'nyh robotov na baze modeli dvigatelya postoyannogo toka [Diagnosing drives of mobile robots based on a DC motor model]. *Intellektual'nye sistemy v proizvodstve [Intelligent Systems in Manufacturing], 16*(4), 114–121. doi: 10.22213/2410-9304-2018-4-114-121. (in Russian).

25. Nikitin, Yu. R., Trefilov, S. A., & Nikitin, E. V. (2019). Identifitsiruemost' modeli privoda mekhatronnogo ustroystva na baze dvigatelya postoyannogo toka po izmeritel'noy matritse [Identificability of the mechatronic device drive model on the DC motor basis using measuring matrix]. *Fundamental'nye i prikladnye problemy tekhniki i tekhnologii [Fundamental and applied problems of engineering and technology],* (4-1), 114-122. (in Russian).

26. Trefilov, S. A., & Nikitin, Yu. R. (2019). Robot drives diagnostics by identifiability criterion based on state matrix. In *Instrumentation Engineering, Electronics and Telecommunications - 2019 : Proceedings of the V International Forum (Izhevsk, Russia, 20-22 Nov., 2019)* (pp. 105-114). Izhevsk, Russia : Publishing House of Kalashnikov ISTU. doi: 10.22213/2658-3658-2019-105-114.

DOI: 10.22213/2658-3658-2020-32-39

A Syntactic Method in Recognizing Unidentified Objects

N. I. Sidnyaev, Yu. I. Butenko, E. E. Bolotova

Department of Higher Mathematics,
Bauman Moscow State Technical University, Moscow, Russian Federation
E-mail: Sidnyaev@yandex.ru

Received: June 12, 2020

Abstract. The paper deals with the formation of contextual grammars in the methods of complex scene recognition. It proposes the use of multi-level grammar, which includes the task of syntactic analysis of image sequences and the task of syntactic analysis of a scene taking into account the multi-level movement of objects. It is shown that the formation of grammar, describing both the structural information of the image and the interaction of images, is associated with the need to develop an algorithm to output grammar on a given set of dynamic images, which represent a learning sample. As a result of training, structural descriptions of images and descriptions of their relations are formed and later used for syntactic analysis of complex structure events. It is postulated that for dynamic scenes with multi-level movement and complex structure, which is constantly changing in time, it is reasonable to apply context grammar rules, and in this connection arises the concept of multi-level context grammar. Some basic principles of the theory of formal grammars inherent in structural methods of recognition are described.

Keywords: recognition, formal grammar, syntactic method, sign, evaluation, solution, image

INTRODUCTION

Computer vision is one of the most demanded directions in the field of intellectual systems, including complex algorithms of recognition and complex mechanisms of deep machine learning. Computer vision is based on the reproduction of a complex human vision system, allowing to obtain significant information from images, video and other visual means, as well as take the necessary measures or make recommendations based on the information obtained.

Problems appeared in solving problems of image recognition led to the development of various recognition algorithms, one of which is a structural method, also called linguistic or syntactic method [1, 2]. Its peculiarity consists in the fact that the priori descriptions of classes are structural descriptions - formal constructions, in obtaining of which the principle of taking into account the hierarchy of the object structure and the relations existing between the individual elements of this hierarchy within and between the same levels is consistently carried out [3, 4]. The syntactic method of recognition allows to use for the object description the methods of combinatorial regularity of structures, which consist in the fact that operating with a very limited number of atomic (non-derivative) elements and a limited number of rules of

combination, it is possible to obtain a significant variety of descriptions with the help of unlimited (for example, recurrence) application of the rules of combination to the original elements. To build such rules it is possible to apply the theory of formal grammar. In the course of image recognition such elements of the object as subimages, which in turn are divided into more simple subimages and which are in some relations with other subimages, are allocated. This allows to present information about the object in the form of a hierarchical structure, most often with the help of a graph in the nodes of which there are subimages, and arcs indicate the relationship between the selected subimages of the recognized object, as shown in Fig. 1.

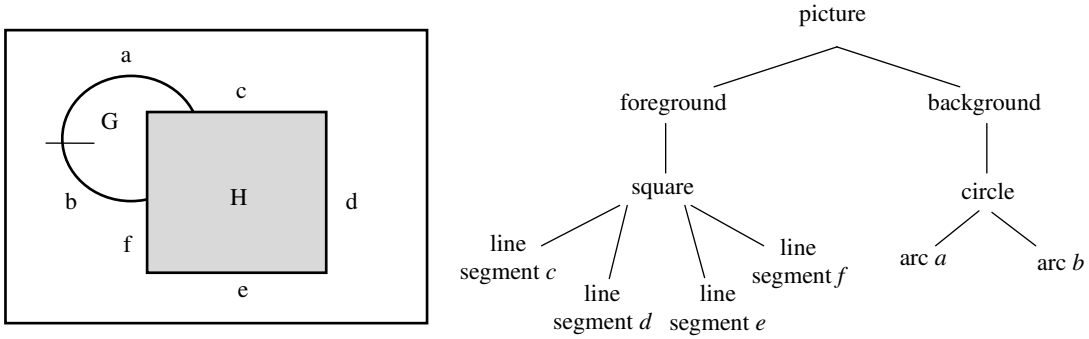

Figure 1. Syntactic image analysis

Within the context of the syntactic approach the decision of a recognition problem is reduced to use of the linguistic constructions containing some dictionary of the recognized object signs and grammar according to which rules elements of the given object are described. Once each subimage inside the object has been identified, the recognition task is realized by performing a syntactic analysis of a sentence describing the object as a tree structure in order to determine whether the sentence is syntactically correct with respect to the grammar indicated. Sentence templates are defined as sequences to be built from selected subimages in different ways, just as sentence phrases are built by concatenation of words and words by concatenation of morphemes. The syntactic approach to image recognition makes it possible to describe many subimages using small sets of simple formal grammar rules [3, 5].

BASIC CONCEPTS OF FORMAL GRAMMAR

Since the implementation of structural methods of pattern recognition is based on the apparatus of formal grammar, we consider some of its basic concepts needed to understand the essence of the structural approach.

The theory of formal languages as a separate discipline usually originates from the studies of the famous American linguist Noam Chomsky, when in the 1950s he attempted to give an exact and unique characteristic of the structure of natural languages. His aim was to define the syntax of languages using simple and precise mathematical rules. It was later discovered that the syntax of programming languages could be described using one of Homsky's grammar models called free-context grammar [6].

In formal language theory, grammar G is a set of rules for generating strings in the formal language. The rules describe how to generate strings from the language alphabet that are valid according to the language syntax. The alphabet is a finite non-empty character set. It is assumed that the characters are indivisible. The word (string) in the alphabet Σ is a finite se-

quence of elements. The generating grammar G is defined as a production system consisting of an ordered set of four elements $G = < T, N, I, P >$, where T is a set of terminal characters of the alphabet Σ, i.e. source elements of the dictionary, N is a finite set of nonterminal (auxiliary) characters, I is the initial character of the grammar and P is the finite set of rules.

The construction of grammar begins with the initial symbol I. By applying the rules first to I and then recursively to the result of the previous transformation, it is possible to generate a correct "sentence" of the formal language defined by grammar. Grammar is built using special substitution rules - expressions of the form "$x \rightarrow y$", which means "substitute x for y" or "substitute x instead of y", where x and y are chains containing any terminal or non-terminal characters. The transformation algorithm stops when the expression no longer contains any nonterminal characters of the alphabet. Thus, according to the rules of grammar, the object is represented by a sentence in this language. To further describe the process of generation it is necessary to introduce such concepts as direct deducibility, deducibility and language generated by grammar [6, 7].

It is important to note that a properly constructed grammar should not contain useless and unattainable symbols.

Definition. The symbol X is called useful in grammar $G = \{T, N, I, P\}$, if there is an output $A \Rightarrow^* \alpha X \beta \Rightarrow^* w$, where $w \in N^*$.

It should be noted that X can be both a variable and a terminal, and the output chain $\alpha X \beta$ is the first or the last in the output.

Definition. If the symbol X is not useful, it is called useless. Obviously, the exclusion of useless characters does not change the grammar generated language, so all such characters can be removed.

Definition. The symbol X is called generating in the grammar $G = \{T, N, I, P\}$, if there is the output $X \Rightarrow^* w$, where $w \in N^*$.

It should be noted that each terminal is a generating symbol, as it is output from itself in 0 steps.

Definition. The symbol X is called achievable in grammar $G = \{T, N, I, P\}$, if there is output $A \Rightarrow^* \alpha X \beta$ for some α, β.

A useful symbol, as the definition suggests, is both generating and achievable. If you remove the non-generating and then unachievable symbols from the grammar first, only useful symbols will remain.

Implementation of the Recognition Process Based on Structural Methods

In order to recognize an unidentified object on the basis of structural methods, it is necessary first to find its non-derivative elements and the relations between them, and then to determine with the help of syntactic analysis (grammatical parsing) whether the description of the image is consistent with the grammar, which, presumably, could have generated it.

To form the appropriate grammar it is possible to use either a priori information about recognized objects, or the results of the study of the final selective set of "typical" in some sense objects. In the first case they speak about the grammar task on the basis of heuristic considerations, in the second case – about the grammar output.

The practical use of the structural method of recognition requires solving the following main problems:

1) construction of the appropriate description of recognized objects;

2) the choice of grammar;

3) implementation of the recognition process through syntactic analysis procedures;

4) the use of training procedures for grammar output;

5) the application of procedures from other recognition methods (e.g. statistical to account for random interference and distortion, cluster analysis, etc.) within a structural approach.

Consider the basic techniques used in the practical application of structural recognition methods.

Methods of mathematical morphology

An important part of image recognition process based on structural methods is the preliminary processing of the analyzed image. At the pre-processing stage the object submitted for recognition is subjected to encoding and filtering, restoring and improving the image quality. Such filtration methods are considered in the framework of mathematical morphology, which provides an effective approach to the analysis of digital images [8, 9]. Morphological filtering does not use analytical parameters of signals, but their geometrical characteristics. The object is encoded or approximated in such a way that it is convenient to work with it further. For example, a black and white image can be encoded using a grid (or matrix) of zeros and onez. To improve the efficiency of processing at subsequent stages of work, at this stage often resort to some kind of "data compression". Then, using filtering and restoration methods, distortion is eliminated in order to improve image quality. It is assumed that at the end of the preprocessing stage, images of sufficiently good quality are reproduced.

Selection of non-derivative elements

The first step in building a structural description of the recognition object is to define a set of non-derivative elements with which to describe the considered object. This choice depends on the nature of the object, the type of source data, the application area and the way the recognition system is implemented in practice. At present, there is no universal solution to the problem of selecting non-derivative elements.

Criterion 1. Non-derivative elements shall serve as the main elements of the image so as to provide a compact and relevant description of the source data by means of well-defined structural relations (e.g., connection relations).

Criterion 2. Non-derivative elements shall be easily distinguishable or recognizable by known nonstructural techniques, as they are assumed to be simple and compact images, which "internal" structural information is not taken into account.

Example. Consider that it is necessary to be able to distinguish rectangles of different sizes from other shapes. The following set of non-derivative elements is selected: a' – 0° – horizontal line segment; b' – 90° – vertical line segment; c' – 180° – horizontal line segment; d' – 270° – vertical line segment. A set of all possible rectangles (different sizes) is defined using a single sentence – a chain $a'b'c'd'$ (Fig. 2). If it is necessary to distinguish between rectangles of different sizes, the given description is inappropriate. In this case it is necessary to use segments of unit length as non-derivative elements. Many rectangles of different sizes can be described using the language:

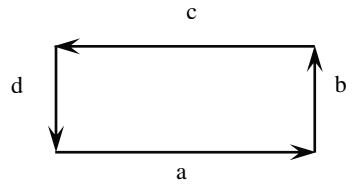

Figure 2. Example for describing a rectangle

$$L = \{a^n b^m c^n d^m,\ n, m = 1, 2, \dots\}.$$

Criterion 2 for the selection of non-derivative elements may in some cases conflict with criterion 1 because non-derivative elements selected under the latter may be difficult to recognize using currently known methods. However, criterion 2 permits the selection of sufficiently complex non-derivative elements as long as they can be recognized. The complexity of the non-derivative elements allows for simplified structural descriptions, i.e. less complex grammar. Finding a compromise solution is essential when building real recognition systems based on the use of structural methods.

Use of grammars and languages for structural description of objects

As already mentioned, grammar can be used to generate proposals that represent an object and to conduct grammatical analyses of proposals to determine whether their structure is acceptable from the point of view of the grammar concerned.

Example. Consider the grammar $G = \{T, N, I, P\}$, where $T = \{a, b, c, d\}$; $N = \{I, A, B, C, D\}$;

$$P: \quad I \to aA \quad A \to b \quad I \to cC \quad C \to d$$

$$I \to bB \quad B \to c \quad I \to dD \quad D \to a$$

In this case four sentences can be displayed ($\Rightarrow$ – output symbol):

$$I \Rightarrow aA \Rightarrow ab; \quad I \Rightarrow cC \Rightarrow cd;$$

$$I \Rightarrow bA \Rightarrow bc; \quad I \Rightarrow dD \Rightarrow Da.$$

If we consider the oriented segments shown in Fig. 2 as non-derivative elements, we can use this grammar to obtain four descriptions of segments forming a right angle. Here we use a technique that allows to describe two-dimensional objects using chain grammar. This method consists in joining the structures only in special points. One of the ways to implement this requirement is that in each structure only two points are selected. In this case, the selected points are interpreted as the beginning and end of the arrow.

Output trees

In the field of computer science the tree is understood as a widely used abstract data type, similar to the hierarchical structure of the tree, with a root value and subtrees - branches with a parent node represented as a set of related nodes [10, 11]. Each tree node has a certain degree that characterizes the number of node subtrees. A node with zero degree is called a leaf. Leaves are nodes from which no branch comes out.

Recognition procedures related to the use of decision trees belong to the group of structural methods, although in the strict sense of the word decision trees are an instrument of hierarchical method of division [11]. The latter is used in cases when the solution tree "contains" many attributes. In each node of the tree one attribute is studied and, depending on the results of this study, the next tree branch is determined. The result of classification is determined at the lower tier of the tree. Such a recognition scheme is very convenient for taking into account a priori information about objects, but it lacks optimal training procedures.

IMPLEMENTATION OF THE RECOGNITION PROCESS USING GRAMMATICAL PARSING

The importance of formal grammars for recognition involves, in particular, the fact that they allow us to speak about the syntactic correctness or incorrectness in relation to a particular grammar representation of the studied image using given non-derivative elements and relations. The answer to this question allows to obtain a grammatical parse procedure [12]. Two

main types of grammatical parse are used: top-down parse and bottom-up parse. The top-down parse procedure consists of consecutive attempts to obtain a given terminal sentence based on the initial symbol by using the rules of corresponding grammar. When using the bottom-up parse procedure, it is necessary to restore the output tree starting from the elements of the main dictionary and applying inverted substitution rules. This procedure starts with a specific sentence and ends when the initial character is obtained.

It is necessary to form a grammar such that when introducing into the grammar analyzer any of the given objects and parsing it according to the received grammar one or several structural descriptions of the object are reproduced at the analyzer output. Then the grammar conversion procedure is performed:

1. All excessive rule entries are eliminated if a rule enters the transformable G grammar several times.

2. Such a pair of auxiliary dictionary elements are found, that identification of these elements (replacing one with another in the whole grammar) will lead to excessive rule occurrence. If there are different options for selecting such pairs, the pair leading to the largest number of redundant occurrences should be selected. After identification of the rules it is necessary to return to step 1.

3. Such a pair N, n is found, which includes an element of the auxiliary dictionary N and a non-derivative element n, that the inclusion of the rule $N \rightarrow n$ in the grammar G (if it is not included in it) and the selective substitution of N by n in the grammar G result in the reduction of the number of the rules after the elimination of the multiple occurrences. If there are different variants of choice of such pairs, it is necessary to choose the pair providing the greatest reduction of the number of rules in grammar. Then it is necessary to return to step 1.

4. The thresholds are entered according to the number of rules to be identified in steps 1-3: replacement is performed if the number of occurrences or the rules to be identified are not less than the threshold value. It is done in order not to decrease essentially dividing force of grammar.

5. A threshold is introduced for the number of rules that are identical in everything (the exception is the type of the non-derivative element): if the number of such rules is greater than or equal to the value of the threshold, the corresponding rules are replaced by one containing a non-derivative element of any type. We should then return to step 1.

If further simplifications are not possible, the procedure is terminated. The result is one grammar. After the specified procedure is performed for each of the grammar formed in the first step, it is necessary to choose the "best" grammar. For example, the ratio of the separating force of the grammar to the square of the number of its rules can be used as the criterion of optimality of the grammar, and the separating force of the grammar is defined as the sum of separating forces of each of its rules; the latter is defined as the sum of the number of non-derivative elements and the number of terms representing a relation or a property.

CONCLUSION

In this paper the syntactic method for recognition of multilevel and poorly structured objects is considered. It is postulated that in order to recognize an unidentified object on the basis of structural methods, it is necessary first to find its non-derivative elements and relations between them, and then to determine with the help of syntactic analysis whether the description of the image is consistent with the grammar, which, presumably, could have generated it. Each object is treated as a chain or sentence because it is composed of elements of the main dictionary. The grammars presented can be used to classify objects, since the presented unidentified object can be attributed to a certain class if it is a sentence of a language. Otherwise,

the object is attributed to another class. As a rule, the object is enrolled to the class in whose language it appears to be a grammatically correct sentence. If the last sentence is not executed, it is obvious that the object does not belong to any of the specified classes and, therefore, one more grammar is required, etc. The object to be recognized belongs to the class of interest in that and only if it is a grammatically correct sentence of the language.

As a criterion of optimality of grammar can be used, for example, the ratio of the separating force. Words can be combined into more complex structures – sentences. Here language is considered as a set of sentences. Suggestions are built from words and simpler sentences according to syntax rules. The syntax of the language is a description of the correct sentences. Alphabet, vocabulary and syntax fully define a set of acceptable language constructs and internal relationships between constructs. The set of syntax rules forms the grammar of the language. Syntax rules can describe either the procedure for receiving correct sentences or the procedure for recognizing the "correctness" of sentences (i.e. their belonging to the given language). In the first case the grammar will be generating, in the second case – recognizing. Criterion for the choice of method may be the simplicity of determining the measure of proximity, the complexity of writing off the boundaries of classes and images, resolution, etc. Thus, it is very important to consider the individual physical features of recognizable objects, informativity of the chosen attributes, quantity and quality of the a priori and current information, possibility of entering of adaptation (weight) factors, etc.

REFERENCES

1. Vasendina, I. S., Aleshko, R. A., Gur'ev, A. T., Karlova, T. V., & Shoshina, K. V. (2017). Razrabotka metodiki raspoznavaniya obrazov na izobrazhenii na osnove strukturnogo podhoda [Procedure development for image identification on picture based on structural approach]. *Bulletin of the Bryansk State Technical University*, (1), 171-177. doi: 10.12737/24908. (in Russian).
2. Prokof'eva, E. V., & Prokof'eva, O. Yu. (2018). Klasternyj, korrelyacionnyj i strukturnolingvisticheskij metody v raspoznavanii obrazov [Cluster, correlation, and structural-linguistic methods in pattern recognition]. In *Sovremennye issledovaniya v sfere estestvennyh, tekhnicheskih i fiziko-matematicheskih nauk [Modern research in the field of natural, technical and physical and mathematical sciences]* (pp. 679-685). Kirov, Russia : Interregional center for innovative technologies in education. (in Russian).
3. Haustov, P. A. (2017). Algoritmy raspoznavaniya rukopisnyh simvolov na osnove postroeniya strukturnyh modelej [Algorithms for handwritten character recognition based on constructing structural models]. *Komp'yuternaya optika [Computer Optics], 41*(1), 67-78. (in Russian).
4. Sidnyaev, N. I., Butenko, Yu. I., & Bolotova, E. E. (2019). Ekspertnaya sistema produkcionnogo tipa dlya sozdaniya bazy znanij i konstrukciyah letatel'nyh apparatov [Rule-based expert system for creating a knowledge base on aircraft structures]. *Aviakosmicheskoe priborostroenie [Aerospace Instrumentation]*, 6, 38-52. (in Russian).
5. Singh, M., Khan, H., & Gupta, R. (2018). Digital image processing a formal grammar approach. *International Journal for Research in Applied Sciences and Biotechnology (IJRASB), 5*(2), 3-5. Retrieved from https://www.ijrasb.com/ojs/index.php/ojs-ijrasb/article/view/44.

6. Hodzhabekyan, M. S., Avramenko, A. A., & Zejtunyan, V. M. (2017). Porozhdayushchaya grammatika N. Homskogo [N. Chomsky's generating grammar]. In *Razvitie nauki i tekhniki: mekhanizm vybora i realizacii prioritetov. Chast' 5. [Development of science and technology: a mechanism for selecting and implementing priorities. Part 5]* (pp. 92-94). Ufa, Russia : Aeterna. (in Russian).
7. Glushkov, V. M. (1961). The abstract theory of automata. *Russian Mathematical Surveys, 16*(5), 1-53. doi: 10.1070/RM1961v016n05ABEH004112. (in Russian).
8. Vizil'ter, Yu. V. (2008). Obobshchennaya proektivnaya morfologiya [Generalized projective morphology]. *Komp'yuternaya optika [Computer Optics], 32*(4), 384-399. (in Russian).
9. Shashev, D. V., & Shidlovskij, S. V. (2015). Morphological processing of binary images using reconfigurable computing environments. *Optoelectronics, Instrumentation and Data Processing, 51*(3), 227-233. doi: 10.3103/S8756699015030036. (in Russian).
10. Sidnyaev, N. I. (2016). *Nejroseti i nejromatematika [Neural networks and neuromathematics]*. Moscow : Bauman Moscow State Technical University, 83 pp. (in Russian).
11. Finogeev, A. G., & Chetvergova, M. V. (2012). Razrabotka i issledovanie metodiki raspoznavaniya izobrazhenij dlya sistem rasshirennoj real'nosti [Development and research of image recognition techniques for augmented reality systems]. *Izvestija volgogradskogo gosudarstvennogo tehnicheskogo universiteta [Izvestia VSTU]*, (15), 130-136. (in Russian).
12. Favorskaya, M. N., & Goroshkin, A. N. (2008). Model' raspoznavaniya izobrazhenij rukopisnogo teksta [The invariant model for image recognition of hand-written text]. *Vestnik of SibGAU*, (2), 52-57. (in Russian). Retrieved from https://vestnik.sibsau.ru/en_US/vestnik/929/.

Serial scientific electronic edition

"INSTRUMENTATION ENGINEERING, ELECTRONICS AND TELECOMMUNICATIONS - 2020"

Proceedings of the VI International Forum
(Izhevsk, Russia, December 2-4, 2020)

Internet address:
http://ieet.istu.ru/proceedings/IEET-2020.pdf

Date of web publishing: 03.12.2020

Technical editor *S. V. Zvyagintsova*
Proofreader *I. V. Ganeeva*
Layout by *N. V. Paklina*
Cover design by *K. Sabour*

Signed to use on November 26, 2020. Size: 4.1 Mb. Order No. 216
Publishing House of Kalashnikov Izhevsk State Technical University
Studencheskaya St. 7, 426069 Izhevsk, Russia

Продолжающееся электронное научное издание

«ПРИБОРОСТРОЕНИЕ, ЭЛЕКТРОНИКА И ТЕЛЕКОММУНИКАЦИИ – 2020»

Сборник статей VI Международного форума
(Россия, Ижевск, 2–4 декабря 2020 года)

Адрес в информационно-телекоммуникационной сети:
http://ieet.istu.ru/proceedings/IEET-2020.pdf

Дата размещения на сайте: 03.12.2020

Технический редактор *С. В. Звягинцова*
Корректор *И. В. Ганеева*
Верстка *Н. В. Паклиной*
Дизайн обложки *К. Сабура*

Подписано к использованию 26.11.2020. Объем 4,1 Мб. Заказ № 216
Издательство Ижевского государственного технического университета
имени М. Т. Калашникова. 426069, Ижевск, Студенческая, 7